

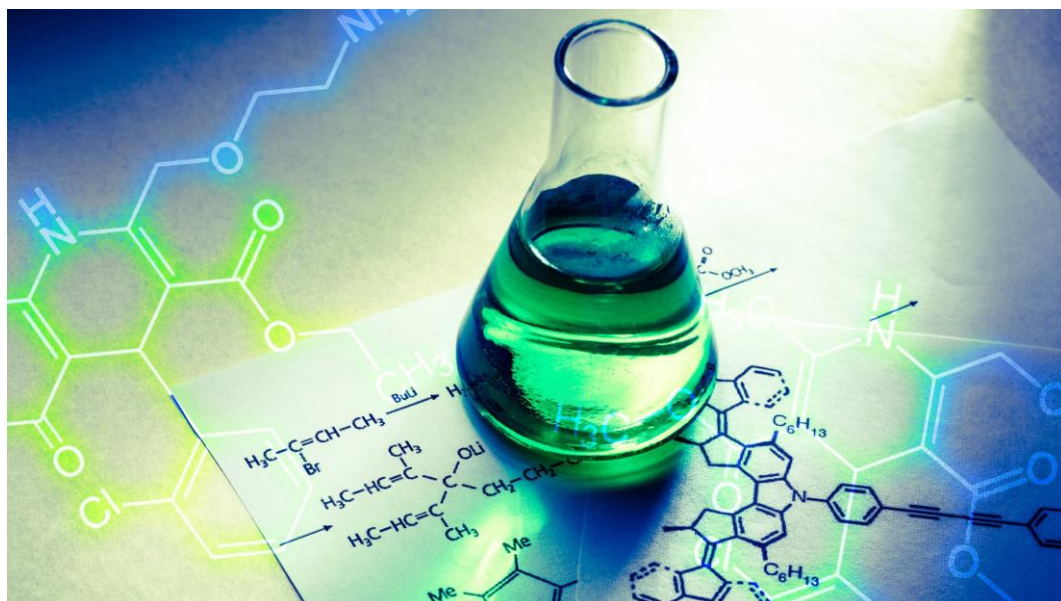
A NOVEL INDUSTRIAL BIOTECHNOLOGY PATH TO VALORIZE FATTY ACIDS: SCOPE TO SCALE- UP AND BUILD PROCESS AND EFFICIENCY.



National Technical University of Athens

School of Chemical Engineering

Department of Process Analysis and Plant Design (II)



Pantelis Vasilakis, Athens, 2023

ACKNOWLEDGEMENTS

Words cannot express my gratitude to my professor, Dr. Antonis Kokossis, Professor in the School of Chemical Engineering National Technical University of Athens (NTUA) in the department of Process Analysis and Plant Design, who provided me with invaluable guidance and enthusiasm throughout the whole study.

This diploma thesis would not have been possible without the contribution of Dr. Konstantinos Pyrgakis, PhD in Chemical Engineering (NTUA), who generously provided knowledge and expertise through all the stages of the thesis.

I would like to extend my sincere thanks to Antonino Biundo, PhD, who constantly contributed his valuable knowledge with perfect cooperation.

Lastly, I would like to thank my family and friends who persistently provided me with the support I needed.

ABSTRACT

From industrial facilities to households, a vast amount of waste is generated every year at an alarmingly higher rate. Nowadays, the amount of global waste is on the rise creating a chatter amongst the academic and industrial community as to what measures could be taken to possibly address this phenomenon. Mismanaged or untreated waste imposes a dramatic impact on ecosystems, climate change and consequently on human health.

Waste cooking oils have great potential as raw materials for industrial high-value products such as bioplastics and biodiesel. Today, advances in technology allow the utilization and valorization of such cooking oils using different kinds of processes. Frying oils can be treated with saponification to produce soaps for dishwashing purposes, while purification methods of valorization of such oils could lead to plasticizers, bio-lubricants, polymers or even biodiesel.

This study illustrates a novel WCO valorization chemistry for the production of added-valued bioplastics. The core process is based on bio-based catalysis, in which *E.Coli* is fermented to produce oleate hydratase enzyme, which catalyzes the conversion of FFAs into the key building block of 10-Hydroxystearic-Acid (10-HA). The core process is further integrated with upstream saponification-acidification stages for the pre-treatment of mixed WCOs, while downstream chemical processes (hydrogenation, esterification, polymerization) are upgrading the 10-HA building block into bio-based poly-10-HAME polymer.

A Techno-Economic Analysis is necessary to ensure the viability of the proposed biorefinery plant conceptual design, by calculating the capital and operational expenditures. The sustainability of this novel chemical approach is provided by employing energy integration and Life Cycle Assessment practices to further establish a decrease in the overall energy consumption and a more environmentally friendly approach respectively.

ΠΕΡΙΛΗΨΗ

Σήμερα, παγκοσμίως παράγεται μία μεγάλη ποσότητα ελαίων τηγανίσματος, τα οποία συχνά απορρίπτονται στο περιβάλλον υποβαθμίζοντας την ποιότητα του εδάφους, μολύνοντας τον υδροφόρο ορίζοντα και κατά συνέπεια την ποιότητα του οικοσυστήματος και την ανθρώπινη υγεία.

Τα απορρίματα ελαίων μπορούν να αξιοποιηθούν για την παραγωγή χρήσιμων βιομηχανικών προϊόντων όπως πλαστικοποιητές, βιοπολυμερή και βιοντίζελ. Πρόσφατες τεχνολογικές εξελίξεις, επιτρέπουν την αξιοποίηση τέτοιων ελαίων με μεθόδους όπως η σαπωνοποίηση και η βιοκατάλυση.

Η παρούσα διπλωματική εργασία προτείνει έναν καινοτόμο χημικό σχεδιασμό ενός βιοδουιλιστηρίου για την παραγωγή ενός ωφέλιμου βιοπολυμερούς. Η βασική διεργασία χρησιμοποιεί το βακτήριο *Escherichia Coli* για την παραγωγή ενός ενζύμου το οποίο καταλύει με μεγάλη εκλεκτικότητα την αντίδραση μετατροπής των FFAs (καθαρισμένα έλαια) στα ζητούμενα 10-HAs. Για την παραγωγή του ζητούμενου προϊόντος (10-HA) απαιτείται διεργασία σαπωνοποίησης για την αναβάθμιση (καθαρισμός) των ελαίων πριν πραγματοποιηθεί το στάδιο της βιοκατάλυσης. Στη συνέχεια λαμβάνουν χώρα διεργασίες υδρογόνωσης, εστεροποίησης, απόσταξης και πολυμερισμού προκειμένου να παραχθεί το ζητούμενο βιοπολυμερές (poly-10-HAME).

Για την ολοκλήρωση του σχεδιασμού του βιοδουιλιστηρίου πρακτικές όπως η τεχνοοικονομική ανάλυση έχουν εφαρμοστεί για να αξιολογηθεί το οικονομικό κόστος του εγχειρήματος υπολογίζοντας τις κεφαλαιουχικές και λειτουργικές δαπάνες. Η βιωσιμότητα της διεργασίας αποτυπώνεται επίσης από την αξιολόγηση του κύκλου ζωής (LCA) καθώς και από τον ενεργειακό σχεδιασμό του βιοδουιλιστηρίου, με απώτερο σκοπό την προφύλαξη του περιβάλλοντος και την μείωση των ενεργειακών απαιτήσεων αντίστοιχα.

TABLE OF CONTENTS

ACKNOWLEDGEMENTS.....	3
ABSTRACT.....	4
ΠΕΡΙΛΗΨΗ.....	5
TABLE OF CONTENTS.....	6
LIST OF FIGURES.....	8
LIST OF TABLES.....	9
1 INTRODUCTION.....	10
1.1 MOTIVE FOR THESIS/ INTRODUCTION.....	10
1.2 BIOREFINERIES AND MICROBIAL FERMENTATION	12
1.3 WASTE COOKING OILS	13
1.4 BIO-CATALYSIS	14
1.5 CHEMICAL PROCESS DESCRIPTION	15
1.5.1 Saponification- Acidification (pre-treatment).....	16
1.5.2 Bio-Catalysis: E. Coli to produce compound	17
1.5.3 Hydrogeneration- Esterification.....	17
1.5.4 Distillation	19
1.5.5 Polymerization	20
1.6 EXPERIMENTAL DATA.....	20
1.7 METHODOLOGY OF THE CHEMICAL PROCESS	23
1.7.1 Process Flow Sheeting.....	23
1.7.2 Process Modelling.....	24
1.7.3 Sensitivity Analysis	25
1.7.4 Energy Integration	26
1.7.5 Life Cycle Analysis	26
1.7.6 Techno-economic Analysis.....	27
2 RESULTS OF COMPUTATIONAL ANALYSIS.....	28
2.1 BIO-CATALYSIS DESIGNING	28
2.2 KINETIC MODELS OF BIO-CATALYSIS.....	30
2.2.1 Bio-catalysis producing the enzyme	30
2.2.2 Enzymatic conversion of FFAs.....	37
2.3 UPSTREAM AND DOWNSTREAM PROCESSES	40
2.3.1 Saponification-Acidification	40
2.3.2 Bio-catalysis.....	42

2.3.3	Hydrogeneration	43
2.3.4	Esterification	44
2.3.5	Distillation	45
2.3.6	Polymerization	46
2.4	ASPEN PROCESS MODELS	47
2.5	WHOLE CHEMICAL PROCESS.....	50
2.6	RESULTS.....	51
2.7	SENSITIVITY ANALYSIS.....	51
2.8	ENERGY INTEGRATION.....	53
2.9	LIFE CYCLE ANALYSIS.....	54
2.10	TECHNO-ECONOMIC ANALYSIS.....	56
3	CONCLUSIONS.....	58
	SUGGESTIONS & FUTURE WORK	59
	REFERENCES.....	60
	APPENDIX A: PROCESS SIMULATION	64

LIST OF FIGURES

Figure 1.1: Valorization applications of WCOs [13]	11
Figure 1.2: Waste management preferability order [11].....	11
Figure 1.3: Concepts of manipulating WCOs [36].....	14
Figure 1.4: Schematization of the saponification step using alkaline hydroxides transforming triglycerides into soaps and glycerol.....	16
Figure 1.5: A schematic representation of a catalytic hydrogenation mechanism.....	18
Figure 1.6: Analytical representation of the esterification process, where the double bond in carboxylic acid breaks to conjoint the alcoholic carbon source, consequently producing an ester and water.....	18
Figure 1.7: Three-stage distillation process.....	19
Figure 1.8: Schematic representation of polymerization	20
Figure 1.9: Stages of the biorefinery plant	24
Figure 2.1: Two-stage bio-catalysis reactors.....	29
Figure 2.2: Graph to calculate Monod's constant values	33
Figure 2.3: Kinetic growth of E. Coli strains regarding the concentration of O ₂	35
Figure 2.4: Schematization of kinetic growth regarding temperature	36
Figure 2.5: Schematization of Eadie Diagram to compute M-M constants.....	38
Figure 2.6: Aspen Plus kinetic equations based on the general LHHW form	39
Figure 2.7: Saponification/Acidification steps in Aspen Plus flowsheet.....	40
Figure 2.8: Bio-catalysis part in Aspen Plus flowsheet	42
Figure 2.9: Hydrogeneration process derived from Aspen Plus flowsheet	43
Figure 2.10: Schematization of esterification process in Aspen Plus flowsheet.....	44
Figure 2.11: Aspen Plus flowsheet of the distillation process	46
Figure 2.12: Depiction of the polymerization process derived from the Aspen Plus simulation engine	47
Figure 2.13: Illustration of the whole chemical process in Aspen Plus.....	50
Figure 2.14: Illustration of the whole chemical process in Aspen Plus.....	50
Figure 2.15: Sensitivity analysis that shows the correlation between the amount of glucose needed with the amount of the enzyme produced.....	52
Figure 2.16: 3D Demonstration of the contribution of oleic and linoleic acid in producing 10-HA	52
Figure 2.17: Grand Composite Curve retrieved from the energy integration	54
Figure 2.18: LCA results retrieved from the SimaPro software	56
Figure 3.1: Schematization of the whole chemical process simulation.....	64

LIST OF TABLES

Table 1.1: Compound inlet flow.....	22
Table 1.2: Conditions, time necessity and experimental yield for each stage	22
Table 2.1: Outlet/inlet streams of the first bio-catalysis	28
Table 2.2: Outlet/Inlet streams of the second bio-catalysis.....	29
Table 2.3: Glucose concentration (mmol/l) in association with the time (h)	32
Table 2.4: Kinetic growth rate of E. Coli with respect to oxygen's concentration.....	34
Table 2.5: Temperature's impact on kinetic growth.....	36
Table 2.6: Depiction of calculations for the drawing of Eadie Diagram utilizing literature data.....	37
Table 2.7: Saponification/Acidification process inputs and outputs	41
Table 2.8: Inlets and outlets of the Bio-catalysis stage derived from Aspen Plus process simulation .	42
Table 2.9: Inlets and outlets of the hydrogenation process.....	43
Table 2.10: Inlets and outlets of the esterification process retrieved from the Aspen Plus simulation engine	45
Table 2.11: Main Inlets and outlets of the three-stage distillation process	45
Table 2.12: Primary inlets and outlets of the polymerization process	47
Table 2.13: Comparison between experimental and simulation process yields of the key stages of the whole biocatalytic process.....	51
Table 2.14: Thermal data utilized for the energy integration (Cold streams)	53
Table 2.15: Thermal data utilized for the energy integration (Hot streams)	53
Table 2.16: Inputs of the process simulation to estimate the environmental impact (LCA)	55
Table 2.17: Outputs of the process simulation to estimate the environmental impact (LCA)	55

1 INTRODUCTION

1.1 MOTIVE FOR THESIS/ INTRODUCTION

From industrial facilities to households, a vast amount of waste is generated every year at an alarmingly higher rate. Nowadays, the amount of global waste is on the rise creating a chatter amongst the academic and industrial community as to what measures could be taken to possibly address this phenomenon. Mismanaged or untreated waste imposes a dramatic impact on ecosystems, climate change and consequently on human health. According to the Guardian, mismanaged waste and waste dumping kills up to a million people globally every year [24]. Apart from the environmental footprint caused, unexploited waste could potentially be financially beneficial for biodiesel, polymers or soap production. There has been extensive research on the exploitation of waste, which primarily focuses on solid household or industrial waste. This category includes municipal solid waste, industrial hazardous and non-hazardous, electronic, plastic, biomedical and construction/demolition waste [10]. However, a high percentage of the overall waste generated consists of used vegetable cooking oils, usually referred to as waste cooking oils (WCOs), as well. WCOs are mainly discarded in landfills, finding a way through the ecosystem and imposing great risks on climate change human health. Global waste generation is not a new scenario, it continuously insists on being one of humanity's greatest obstacles. The challenge is shared by both industrialized and developing nations. Even though the attention, on a global scale, for better waste management is increased, the impact still exists causing negative effects for the environment in the future. Overall, mistaken global waste management will impact everyday life in numerous ways.

The high amount of falsely generated WCOs creates the need to study this phenomenon extensively. Traditionally, vegetable cooking oils are being disposed into landfills, drains and syphons resulting in deteriorating damage to the environment. This direct disposal contaminates all kinds of bodies of water leading to potential pollution and eventually the extinction of aquatic life. On top of that, waste cooking oils degenerate the soil quality, hence causing soil pollution. All the above pose a great risk for the eco-system that leads to catastrophic effects on the indigenous flora and fauna. As a result, severely damaging the ecosystem and intervening in the natural food chain would negatively affect human health as well [11].

Waste cooking oils have great potential as raw materials for industrial high-value products. Today, advances in technology allow the utilization and valorization of such cooking oils using different kinds of processes. For instance, waste cooking oil may be utilized as a feedstock for the manufacturing of biodiesel, an ecologically beneficial and renewable fuel that can be used in diesel engines. WCOs are characterized by fascinating properties, since if treated and burnt properly, they can generate high amounts of energy. The exploitation of used cooking oils can be applied for soap manufacturing to form soaps and other hygiene aromatic products, such as candles or cleaning supplies, a field dominant in today's market [12].

WCOs offer a promising path to eliminating global waste and environmental pollution if measures are applied religiously. One way to implement that is explained by the circular economy which states the usage and exploitation of seemingly useless materials to high-value products. *Figure 1.1* depicts today's applications of WCOs attaching with the principals of recycling management and circular economy, reducing pollution and increasing the production lines of numerous industrial fields.

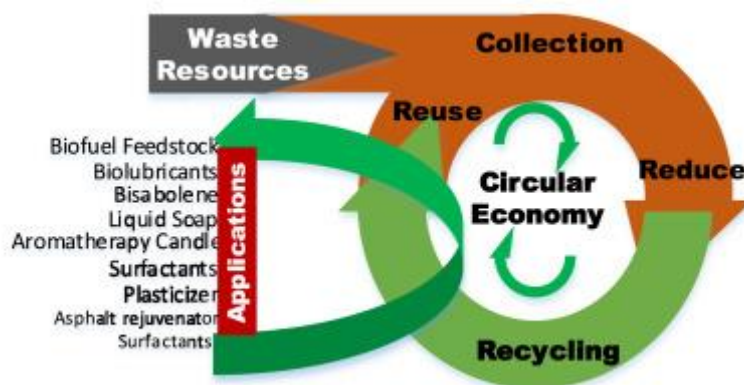


Figure 1.1: Valorization applications of WCOs [13]

Summarizing, WCOs could be a great value carbon source and alternative since there are plenty of industrial pathways that could be followed. Valorising and adding value to waste compounds is the key to achieving circular economy.

The novel chemistry that is being studied is of high importance due to the benefits of producing high-valued products, exploiting recycled raw materials, that otherwise would be mistreated and disposed [1]. The aim of this thesis is to exploit alternative biorefining approaches, valorizing waste cooking oils producing high value-added products. The innovative valorization process assists in decreasing mistreated global waste; thus reducing environmental pollution, seeking sustainable solutions, in line with circular economy and green chemistry. Figure 1.2 illustrates the preferability order of waste, from disposal to prevention, to assist in preventing environmental pollution.



Figure 1.2: Waste management preferability order [11]

The utilization of WCOs is of high importance for a more sustainable future. Hence, the purpose of this study is to present a novel approach on cooking oils chemical manipulation to produce high-value

products such as 10-HAME's polymer by incorporating bio-catalysis reaction and other chemical processes.

1.2 BIOREFINERIES AND MICROBIAL FERMENTATION

Biorefinery by definition is a plant or in general a chemical process or processes that treat biomass in order to produce a spectrum of desired products and energy. There is significant difference between the biorefineries and the traditional refineries. Biorefineries are built to follow a more sustainable approach, seeking solutions in waste management using greener tools exploiting the ideas and the valorization pathways of green chemistry [2]. On the other hand, traditional refineries utilize non-renewable resources such as crude oil, which is finite and continuously depleting. The main concern about traditional refineries is the environmental impact that imposes. Traditional refineries utilize and produce hazardous elements and compounds that increase the volume of greenhouse gas emissions into the atmosphere, leading to environmental pollution.

Biomass is a non-fossil product retrieved from both natural and unnatural (anthropogenic) processes. Naturally, it is synthesized by growing land and water-based vegetation (carbon source) through metabolic processes like photosynthesis. Unnaturally, biomass is produced via applying and processing the above carbon source and occasionally by fermentation techniques [14]. Overall, biomass leads to chemical compounds that contribute to a more sustainable future approach.

In this work, biomass is retrieved from *E. Coli* cells (bacteria), used to exploit Waste Cooking Oils through a biorefinery plant. On the contrary, there are other biorefineries that utilize lignocellulosic waste feedstocks aiming to produce valuable products. Lignocellulosic materials consist of three components, lignin, cellulose and hemicellulose. This kind of biomass is abundant on earth since it is originated from dry material found in agriculture, forests, etc. Residues of such materials provide a cheap and valuable carbon source that could be utilized to upgrade and produce numerous significant compounds [34]. Lignocellulosic biorefineries could be beneficial concerning the produced compounds complying with the laws of circular economy and sustainability, however WCOs biorefineries outweigh the advantages of lignocellulosic biorefineries for several reasons. Lignocellulosic waste is difficult to handle when it comes to logistics, imposing a problem in transportation. In addition, lignocellulosic waste conceals technology limitations as a consequence of conventional processing while facing an unstable and uncertain economic market [35].

Microbial fermentation is a biochemical process that under specific circumstances, depending on the microorganism, results in biomass. The main role of this highly important process is to catalyze or enhance the selectivity of a reaction, resulting in the desired products. This thesis's fermentation process regards a bacteria called *Escherichia Coli* (*E. Coli*). *E. Coli*, is being fermented to produce an enzyme called *hydratase oleate*, which catalyzes the Free Fatty Acids, after the pretreatment with saponification and acidification processes, producing the key component of the whole chemical process, referred as 10-Hydroxyl-Stearic-Acid. The last is being managed throughout many stages to produce the highly valued biopolymer.

1.3 WASTE COOKING OILS

The management and exploitation of waste cooking oils originating from households are in the early stages in the academic and industrial communities. Vegetable oil after frying is usually disposed into landfills, sinks and sewage systems, which imposes high environmental risks. Oils are then introduced into the eco-system downgrading the quality of life by posing a risk for the human health, as well. Damaging the ecosystem could result in irreversible climate condition change that would utterly change human lives all together. Instead of being mishandled, WCOs should be collected to undergo valorization processes to produce or clean high value compounds. There is a variety of valorized carbon sourced products, which contribute to different industrial fields.

Waste cooking oils today can be treated with saponification to produce soaps for dishwashing purposes, while purification methods of valorization of such oils could lead to plasticizers. Aromatic candles, bio-lubricants, polymers or even biodiesel are possible products from the treatment and chemical manipulation of used frying oils.

Due to the increasing consumption of vegetable oils (150 million tons in 2013, more than 200 million tons in 2021) in parallel with the rapidly growing population, there is a high demand for food and energy supply [4]. Numerically, the market size of the WCO industry is estimated to rise more than 50% in market capitalization [3]. It is safe to assume that the proper exploitation of WCOs would significantly contribute to the circular economy for prevalent domains such as polymers and energy supply.

Fat and oil disposal is still underdeveloped due to the complex challenges regarding the collection, storage and quality of such materials since oils present different phases with temperature change and compound composition. This creates an even more complex issue at hand [15]. Lately, there has been a discussion on how to address these issues.

As mentioned above, managing the major problem of disposing the valuable carbon source of WCO could be a useful alternative pathway, not only because of the environmental benefits but also for the high-value produced compounds. In the future, WCOs could be utilized via promising chemical pathways to produce biofuels and biopolymers. Recycling and utilizing the WCOs through valorization technologies also promotes the circular economy. Although the circular economy proposal addresses the majority of solid waste, the recycling of fat waste is still in its early stages because the necessary European Union legislation has only recently been implemented [15]. According to a study drafted by the European Parliament, a collective effort of different agents is necessary to ensure the proper disposal, collection and treatment of waste cooking oils [29]. From producers and consumers to municipal authorities, legislation should be in place. Establishing legal backgrounds would facilitate the elimination of the amount of oils disposed and create a sense of the responsibility for proper management (of waste). This does not come without challenges, since the appropriate authorities should have eco-friendly plans at place and practical solutions for the collection, transportation and utilization of household oil waste.

Figure 1.3 summarizes the fields/concepts in which WCOs are manipulated to produce valorised high valued products.

Even though there is still a huge amount of unexploited raw material that could be utilized, deeper research should be conducted to find more applications and ways to exploit this hazardous but valuable by-product/resource.



Figure 1.3: Concepts of manipulating WCOs [36]

1.4 BIO-CATALYSIS

Catalysis in general, is the process that modifies the rate of a chemical reaction. Typically, the purpose of the catalysis is to accelerate the chemical reaction by adding a substance (catalyser) that does not participate in the chemical reaction. So, catalysis only speeds up the chemical process by enhancing the velocities of the reacted atoms of the reactants [16].

Bio-catalysis refers to a process where a microorganism, such as bacteria, is utilized to transform a chemical through a bio-chemical reaction, into another chemical compound, accelerating it, for industrial purposes [5]. Employing a bio-based compound to catalyse reactions contributes to more sustainable approaches regarding the environmental impact of traditional catalysers. The main advantage of bio-catalysis is that it provides the chemical process, enhanced selectivity over the chemical reactions, assisting in obtaining desired products of high purity. In addition, bio-catalysis is usually processed under mild conditions, otherwise the catalyser would not be able to intervene with the reaction, due to the fact that it is produced by living microorganisms. Using bio-catalysers is a delicate process due to the sensitivity of microorganisms to temperature, pressure and oxygen percentage. Therefore, the conditions of the desired reaction should be handled with caution. In this case, lowering the production costs of the process, decreasing the energy cost by reducing the energy consumption (e.g., Lower temperature and pressure).

It should be noted that bio-catalysis retrieved from the novel chemistry procedure is processed through one specific bioreactor. To elaborate, *E. Coli*'s growth and fermentation to produce the desired enzyme, as well as the utilization of the specific enzyme to convert and upgrade the chemicals to the key products, all happen in the exact bioreactor. This innovative chemistry procedure implies that the overall operating and capital cost would be substantially decreased, as there is a need for less equipment usage.

In this particular case, a bacteria (*E. Coli*), is being fermented to transform into a specific enzyme. This particular enzyme enhances the selectivity of the main bio-chemical reaction of the whole process, producing 10-HAs from FFAs. This stage is the key procedure because the enzyme catalyses oils, assisting the hydroxyl to interact only with the 10th Carbon of the oils, transforming some of the FFAs to the desired product at the phase of the bio-catalysis process.

1.5 CHEMICAL PROCESS DESCRIPTION

The chemical processing obligates the deep understanding of the utilized chemistries as well as the flowsheet processing knowledge derived from the Aspen Plus simulation engine tool. The combination and application of both could lead to an integrated and innovative chemical process, resulting in trusted estimations of chemical yields and possibilities. At start, processing the fundamental flowchart is of the essence, while selecting the appropriate methods and protocols regarding the utilized blocks of Aspen's Plus reactors. Simultaneously, it is necessary to insert data regarding the chemical compounds that are used as reactants, products and in general every chemical compound or element participating in any section of the whole chemical process, employing Aspen Plus data bases. In some cases, rarely utilized compounds were not inserted into the databases, so a chemical structure needed to be extracted or created in order to estimate and establish the known and unknown properties of each compound. In parallel, specifications regarding the processing and the chemical compounds used, need to be clarified. Methods and protocols such as the thermodynamic approach of the chemical system are chosen while estimated from simulation engine tool method assistant providing more realistic and trusted estimations concerning the properties of the whole bio-catalytic process. On top of that, known yields and reactions are embedded into the process analysis tool, together with the knowledge of the chemistries involved, to establish the process modelling flowsheet. This pathway requires critical thinking to be conducted as to what assumptions need to be involved to consequently obtain an integrated and conceptual chemical design. For instance, waste cooking oils consist of numerous acids not only the ones inserted into the simulation. Tiny amounts of different acids were ignored for this study due to their insignificant proportion. On top of that, waste cooking oils, consist of the triglycerides of oleic (triolein), linoleic (trilinolein), palmitic (tripalmitate) and stearic acid (tristearate), where glycerol's carbons connect the above acids respectively, in forms of triglycerides.

On the other hand, bio-catalysis is the most important part of the process, due to the fact that it produces the key component; however, other stages of the process are of high importance, contributing to the whole chemical process. At start, WCOs must go through a pre-treatment process, to disengage the oil carbon chains from the triglycerides. The raw material (WCO), is chemically pre-treated, employing a saponification stage using KOH as a reactant under the influence of ethanol, which is added to accelerate the saponification process [25]. Afterwards, an acidification step is applied to retrieve the oils (FFAs) and remove the potassium element. Simultaneously, the treatment of the catalyst is taking place, to produce the biomass needed for the upcoming stage of bio-catalysis. *Escherichia Coli* cells are being incubated to produce the wanted quantity of biomass which is an enzyme called oleate hydratase. During the simulation processing, glucose is used as a substrate to produce the enzyme that eventually bio-catalyses the FFAs, selectively turning them into the key components (10-HAs), where a small percentage of the resulted acids are in an unsaturated form (double carbon bond). The mixture then undergoes several separation stages necessary for cleaning purposes, such as to remove the add-ins. The enzyme is also retrieved from the exit stream because it imposes malfunctions regarding the simulation estimations. The mixture, that consists of FFAs and 10-HAs is hydrogenated to break the double carbon bonds, to saturate the acids in high purities. Then, there is the esterification process, in which, methanol reacts with the saturated mixture, under the influence of acid catalyst (sulfuric acid) to enhance the yield of the esterification, forming Fatty-Acid-Methyl-Esters (FAME) and more importantly 10-Hydroxyl-Stearic-Acid-Methyl-Ester (10-HAME) [26]. At the end of this stage, the chemicals must be separated, implementing distillation columns. Three distillation columns are embedded to predominantly separate 10-HAME from FAME (Biodiesel).

Other, crucial amounts of secondary chemicals as methanol or ethyl-acetate (that is used for mixing purposes) are being separated and recycled in the bio-chemical plant. The last stage is the polymerization process, in which the saturated-esterified product, reacts in high temperatures in a saturated N₂ environment, to transform into the saturated-polymerized-esterified product, the Poly-10-Hydroxyl-Stearic-Acid-Methyl-Ester (Poly-10-HAME).

Besides the chemical process description, and the results that are obtained regarding yields and different approaches for the used chemicals of a biorefinery plant, excessive analysis concerning the economic approach and environmental impact of such an undertaking is evaluated in the upcoming chapters.

1.5.1 Saponification- Acidification (pre-treatment)

Saponification reaction in general is process where soaps are produced. In saponification, an ester reacts with an alkaline base (usually sodium and potassium hydroxides) to form alcohol and long chains of fatty acids containing potassium or sodium. In some processes, when necessary, after the saponification step, an acidification step is followed to purify the soaps from the adjusted sodium or potassium elements. Strong alcohol reacts with the soaps retrieving salts and free fatty acids.

The pre-treatment of the WCOs is obligatory to break the bonds between the triglycerides that WCO consists of and later to form FFAs retrieved from the fatty acid soaps. In this work, saponification (RSTOIC model) takes place using KOH (5 M) to break the bonds of triglycerides of WCO resulting in glycerol and potassium oleic, linoleic, palmitic and stearic acid. Potassium-FFAs are produced, which are then acidified in presence of H₂SO₄ returning the treated FFAs for bio-catalysis. A vapor-liquid separation stage is employed to recover volatile compounds in acidification effluents, while a downstream decanter is implemented to remove the water-glycerol content finalizing the bio-catalysis feedstock. A schematic representation of the saponification step utilizing an alkaline hydroxide (KOH) transforming triglycerides into soaps and glycerol, is illustrated in *Figure 1.4*.

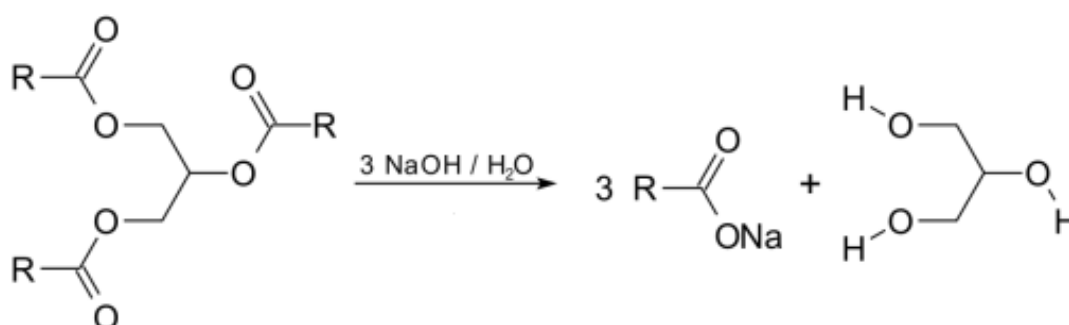
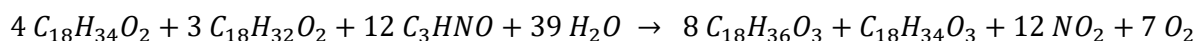
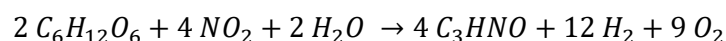


Figure 1.4: Schematization of the saponification step using alkaline hydroxides transforming triglycerides into soaps and glycerol

1.5.2 Bio-Catalysis: E. Coli to produce compound

Escherichia Coli, abbreviated as E. Coli are a wide group of bacteria located in the intestines of humans and animals that secure the intestinal health. They are primarily harmless considering human health, but consuming certain types of E. Coli can consequent to various intestinal illnesses, thus treating and utilizing bacteria in general should be an accountable process [18]. However, exploiting bacteria and microorganisms for fermentation causes opens a wide variety of solution processing leading to valuable and special outcomes. A substantial number of bacteria and biological life generally obtain a charismatic effect to catalyse and enhance the selectivity of specific reactions when fermented and turned into biomass. In this work, E. Coli strains are fermented to produce an enzyme that catalyses the FFAs into 10-HAs. In the process simulation, E. Coli is fermented by consuming glucose resulting in oleate hydratase enzyme. For this cause, an imaginary enzyme was exploited for simulation purposes, to identify as the real produced enzyme. Furthermore, the enzyme contributes to the production of 10-HAs, the key components of the whole chemical process.

To be more specific, the below equations represent the chemical reactions used for the simulation process, producing the enzyme and the key components respectively.



The above experimental equations will be analysed and revised in the upcoming Chapter 2.

Specifically, the biocatalyst was prepared by inoculation to reach 3 tons of biomass ready for use in fermentation (37 °C). In addition, a separation block was employed, used as a membrane to remove some admixtures (e.g., imaginary enzyme) that led to failed simulation results of the Aspen Plus simulation engine. Furthermore, the bio-catalysis exit stream is treated with ethyl-acetate solvent (EtOAc) (5% v/v) to facilitate mixing and extraction of the bio-catalysis phase (desired products) and removal of the excess water content by a centrifugation stage. Next, spray drying was implemented as a three-stream separator, to recover an ethyl-acetate rich phase, the unsaturated FFAs including 10-HAs and the remaining water.

1.5.3 Hydrogeneration- Esterification

Hydrogeneration is one of the most common addition chemical reactions, where a molecular hydrogen (H₂) is reacted with another compound or element. The purpose of this reaction is to saturate organic compounds. This works recovered organic phase, containing FFAs and predominantly 10-HAs is hydrogenated with the use of nickel-based catalyst, utilizing a fixed bed reactor. High temperatures are employed, resulting in breaking the double carbon-carbon bonds, ensuring high percentage of purity. Saturated FFAs are then ready to continue to the next phase. A schematization of a nickel-based catalyst hydrogeneration process is illustrated in *Figure 1.5*.

1.5.4 Distillation

Distillation is a chemical process used for separating purposes in various production lines, employing the different boiling points of the liquids (when liquid-liquid separation occurs). In general, distillation involves a conversion of a liquid into vapor form, separating it from the liquid phase. Then, the vapor condenses into liquid form again due to the slightly lower temperature (form of liquid) at the top of the distillation column, while the other liquid stays intact. Fractional distillation, or differential distillation is another form of distillation which is traditionally employed when boiling points of the separating liquids are in close temperature range (petroleum refining). In this method, the compounds that are distilled (vapours) are continuously condensed into liquid form and then revaporised again to only allow the most volatile compound to exit as a vapor and the less volatile to descend lower in the distillation column [20].

Downstream esterification, a three-distillation system is employed to recover the four key fractions from the ethyl-acetate entrainment:

- (a) EtOAc
- (b) Unreacted MeOH
- (c) FAME
- (d) 10-HAME

The distillation separations have been designed to perform sharp splits at high purities ($\geq 99\%$). Methanol is completely retrieved back in needs of esterification processes always adding the consumed amount needed to esterify the fatty acids, while ethyl-acetate can be recovered back to assist the liquid-liquid separation stages, being completely recycled because EtOAc is limitedly utilized as a mixing and separating enhancer. FAME exit stream constitutes the biodiesel co-product that is then utilized to feed the biorefinery with electrical and thermal energy, reducing the energy cost of the undertaking, while securing the environment. The 10-HAME is finally driven to the polymerization stage producing the poly-10-Hydroxystearic-Acid-Methyl-Ester. The below *Figure 1.7* clarifies the distillation process outcome regarding the separated products.

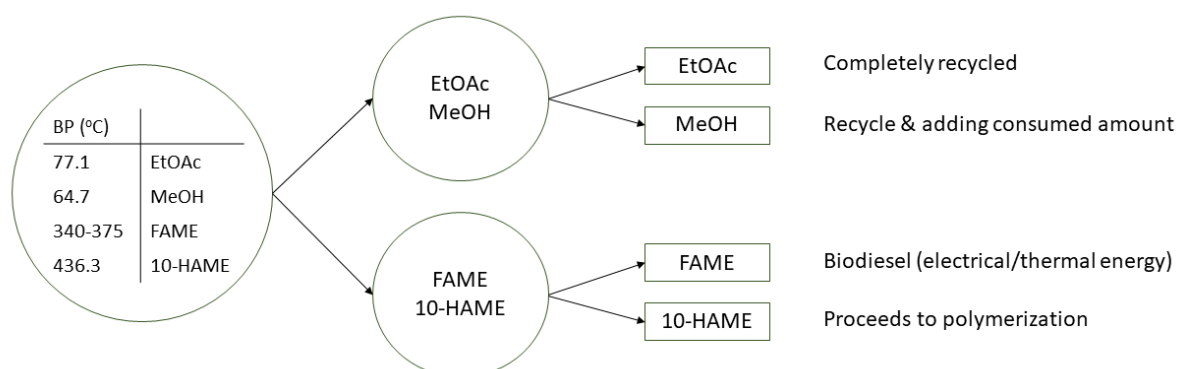


Figure 1.7: Three-stage distillation process

1.5.5 Polymerization

Polymerization is considered any fusion process that utilizes relatively small chemical compounds together called monomers, creating large chemical chains/molecules (macromolecules) called polymers [21]. During the process flow sheeting, after the distillation stage, 10-HAME is fed to a separation block removing any small portion of the overall admixtures to proceed to the polymerization reactor in higher purities, for simulation purposes. The polymerization stage is producing the final key compound of poly-10-Hydroxystearic-Acid-Methyl-Ester (poly-10-HAME) under relatively high temperatures (350°C) for a total of 24 hours in a saturated with nitrogen (N₂) environment for neutrality purposes. The polymerization process takes place under a neutral environment to prevent any interference of oxygen or moisture to the polymerization process, which is an exothermic reaction, thus danger is lurking when employing such reactions. In addition, polymerization process always indicates a use of a catalyst, in this case DiButylTin Oxide (DBTO) was chosen, a catalyst widely used in organic chemistry [22]. When the polymerization process is over, a distillation column is implemented to separate the poly-10-HAME from the unreacted monomers, that are recycled into the next polymerization batch. Below, there is a common polymerization reaction depicting the primal idea of polymerization in *Figure 1.8*.

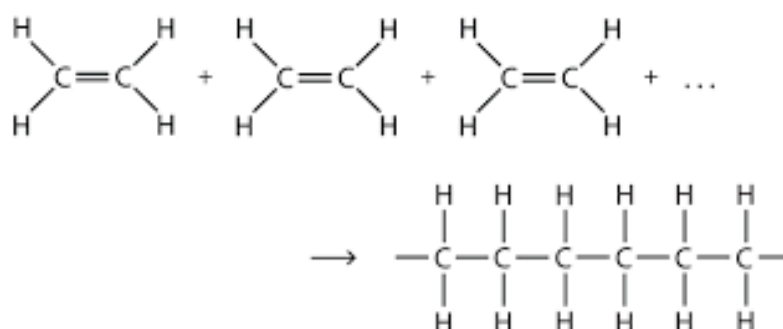


Figure 1.8: Schematic representation of polymerization

1.6 EXPERIMENTAL DATA

This work was conducted in collaboration with bio-catalysis practitioners at REWOW and experimental data were utilized for the preparation and validation of process engineering and modelling of the integrated biorefinery plant. Data regarding the proportions and quantities of each raw material as well as with the conditions of each separate process were taken into consideration.

The starting point of the experimental procedure is the biocatalyst preparation, where 0.788 g of an E. Coli engineered strain is incubated in a flask containing several additives that boost or feed the biomass growth. Subsequently, the grown biomass 31.719 g is transferred to four different bioreactors for a series of consecutive fermentations empowered by mechanical agitation; each one of them, with greater volume than the previous one. The purpose of this successive process is to enable biomass to flourish, under the influence of several culture mediums, until it reaches the desired volume. Next, there is the induction step, where IPTG chemical is added to assist the biomass growth that is later centrifuged to separate the biomass from the liquids of the mixture. Exiting the

centrifugation stage, biomass paste (free from aquatic components) undergoes a downstream washing process to remove any possible contamination. Then, a second centrifugation process is utilized to remove the water phase of the mixture once again to result in the desired amount of whole cell biocatalyst, necessary for the upcoming steps of the bio-chemical process. Continuing to the next laboratory experiment that is the key to the whole chemical process. The organic phase retrieved from the saponification/acidification process is pumped into the bioreactor, where the biomass from the biocatalyst preparation is also inserted into. The bioreactor contains an aquatic solution consisting of several buffers and enhancers for the bio-catalysis step. The process undergoes for 24 h with continuous mechanical agitation to eventually produce the desired compounds. At the end of the bio-catalysis process, the products are pumped, together with an amount of solvent (EtOAc) aiming for complete mixing. After the bioreaction the products are separated utilizing a spray dryer to obtain the recovered EtOAc, which can be recirculated after adding a small amount of fresh solvent, the water phase and the unsaturated FFAs, containing the key components of 10-HAs.

To elaborate on the experimental set-up, for the whole cell biocatalyst preparation, *E. Coli* colonies were incubated utilizing an 100 mL flask followed by a dilution in 2 L flask, while using additives to enhance the fermentation process. The resulted whole cell biocatalyst that is collected is 5 g. For the saponification process, 5 g of WCOs react together with 15 mL (5M) KOH solution to create the soaps that were later enabled to react with 30 mL of a strong acid (HCl) with the addition of 15mL of NaCl (36%). To separate the organic from the water phase a separating funnel was employed, while 100 mL of EtOAc were added for separating purposes. The organic phase was then treated to retrieve the used EtOAc, utilizing a rotary evaporator that recycled the entire 100 mL of EtOAc, resulting in 4.8 g of FFAs. Then, the biocatalyst and FFAs are fused into the bioreactor together with enhancers like NaCitate (482.5 mL) for incubation. After a total of 24 h, 100 mL of NaCl (36%) and 600 mL of EtOAc are added to the bioreactor. The separation of the organic from the water phase occurs in the same manner as previously, collecting approximately 4.8 g of 10-HAs and FFAs. The hydrogenation process was conducted at 50°C and 1 bar for 3 h with the use of catalyst, resulting in around 4.8 g of 10-HA and saturated FFAs. As far as esterification is concerned, 24.5 mL of methanol was employed at 80°C for 24 h with reflux. After the process was completed, methanol is removed through a rotary evaporator, while 50 mL of EtOAc is added once more to assist in solution mixing. Utilizing the same experimental equipment as before, all the amount of EtOAc is evaporated and recirculated, ending up with about 4.8 g of 10-HAME and FAMEs. For the separation of the produced compounds on an experimental scale, a silica gel column was implemented to eventually result is roughly 2 g of 10-HAME and 3 g of FAME. For the polymerization process a dibutyl tin oxide catalyst was utilized under neutral conditions (N₂ environment) to finally produce approximately 1.81 g of the biopolymer.

The below tables (*Tables 1.1, 1.2*) depict the experimental data that was used to illustrate, build and create a completed and integrated process flowsheet utilizing the chemical design tool of Aspen Plus V11. The data was carefully collected and examined through the whole undertaking.

Table 1.1: Compound inlet flow

Compounds inlet (kg/h)	STREAMS								
	1	S2	S7	S8	S11	S19	S20	S23	51
TRIOLEIN	1845								
TRILINOLEIN	753								
TRIPALMITIN	249								
TRISTEARIN	153								
KOH	1800								
WATER	1125	19440		294					48
ETHANOL	7875								
H ₂ SO ₄		13725					1208		
NaCl		5142							
Isopropyl β-d-1-thiogalactopyranoside			18						
BIOMASS (E.Coli)			3000						
TWEEN 20				0.0044					
KANAMYCIN				1					
NaCitrates				271					
H ₂						22			
Ethyl Acetate					1322.53			285	
MeOH							1946		
Flowrate (kg/h)	13800	38307	3018	566.0044	1322.53	22	3154	285	48

The first chemical compounds refer to the triglycerides that WCOs consist of. The percentage of each is derived from experimental data based on the medium consistency of vegetable fried oils. KOH is used for the saponification process and H₂SO₄ is employed for the upcoming acidification process. Ethanol is used as a catalyzer and NaCl assists in separation, for the saponification process. IPTG works as an inducer for the bio-catalysis part. Tween 20, kanamycin and NaCitrates are used as boosters for biomass growth. The conditions of each inlet flow are based on the atmospheric pressure and the ambient temperature.

Table 1.2: Conditions, time necessity and experimental yield for each stage

	STAGES						
	Biocatalyst Production	Saponification	Biocatalysis	Hydrogeneration	Esterification	Distillation	Polymerization
P (bar)	1	1	1	1	1	1	1
T (°C)	37	80	37	150	80	47-514	350
Time (h)	64	2	24	3	24	1	24
Yield (%)	-	96	80	95	95	99	90

Table 1.2 illustrates the conditions (Temperature and Pressure) and the time needed for each stage to complete. Stream numbers can be clarified using the pictures of the fully integrated process flowsheet illustrated in Annex 1.

1.7 METHODOLOGY OF THE CHEMICAL PROCESS

The work of this thesis was mainly based on a 6-step pathway to convert laboratory scale chemistry (experimental data) into a complete process biorefinery flowsheet. The purpose of the simulation is to scale-up the whole biocatalytic process, analyze and estimate the existing data as well as the upcoming results, transforming them into valuable and novel biotechnology concepts. The approach primarily consists of:

- 1) Bio-catalysis kinetic estimations: Experimental data regarding the exploited bacteria for the bio-catalysis (E. Coli), were merged with the generalized kinetic input forms of Aspen Plus providing the work with more trusted kinetic results.
- 2) Process flow sheeting from scratch: Preliminary steps of the biorefinery plant. Laboratory chemistry data turning into a process flowsheet diagram depicting the different stages of the process, utilizing Aspen Plus.
- 3) Simulation and scale-up: Fully upgraded system, demonstrating in detail (conditions, flowrates, etc.) the operations of the process in a realistic perspective.
- 4) Energy Integration: Collecting the energy usage data of all the streams of the biorefinery plant to decrease the energy usage employing the pinch technology.
- 5) Life Cycle Assessment (LCA): Conducted research using software to estimate and manage environmental impact of the whole bio-catalytic plant.
- 6) Techno-Economic Analysis (TEA): Investigating the process from an economical perspective; questioning and analyzing the sustainability and feasibility of the biorefinery plant.

Combining unique techniques and approaches of different fields of chemical processing science led to the upgrading of a laboratory scale concept to a scaled-up biorefinery conceptual design. Evaluated results were obtained and estimated followed by knowledge and results from an energy integral and environmental perspective.

1.7.1 Process Flow Sheeting

One of the most important methods followed by when conceptually designing a chemical project, is to create a process flowsheet. Process flow sheeting demands and combines the majority of the knowledge derived from literature and experimental data as well. It is remarkable to declare that not every process flow sheeting, regarding the same industrial chemical process, is the same. There are numerous pathways to follow in order to complete a correct process flowsheet depicting the desired outcome. Therefore, alterations could occur and occasionally are the key to enrich the designing process leading to alternative and sometimes to more preferred suggestions.

The preliminary stages of bio-catalysis plant consist of WCO pre-treatment and bio-catalysis preparation. WCO feedstock constitute a valuable carbon source composed of unsaturated triglycerides (TGs), collected as wastes after vegetable oil is fried. This stream is chemically treated

employing a saponification reaction. Triglyceride forms of Oleic, Linoleic, Palmitic and Stearic acid react with KOH, resulting in potassium oils and glycerol, under the influence of ethanol accelerating the process. The needs to remove the potassium parts of the compounds compel the acidification step to participate. Utilizing H_2SO_4 , a strong acid, potassium is removed from the structures, creating oleic, linoleic, palmitic and stearic acid. The organic phase is later separated from the water phase, ready to participate in the bio-catalysis reaction stage. *Escherichia Coli* bacteria is fermented with culture medium utilizing several add-ins like IPTG (Isopropyl β -D-1-thiogalactopyranoside) that induce and enhance the biomass growth. Glucose, reacts, producing *oleate hydratase* enzyme to catalyse and enhance the selectivity of bio-catalysis. Biomass then reacts with the organic phase (containing the treated oils) in a bio-catalytic reactor transforming oleic and linoleic acid of the total of FFAs into 10-Hydroxyl-Stearic-Acids (10-HAs). Ethyl Acetate (EtOAc) is pumped to assist in mixing purposes to later improve the separation. The following step is the centrifugation to separate the organic from the water phase. A spray drier is also imbedded in the system to recover the auxiliary EtOAc, the unsaturated FFAs that did not react and the water. The stream containing the key components (10-HAs) and FFAs is then hydrogenated in high temperature to break the carbon-carbon bonds. The main goal is to saturate 10-HAs in high purities. Moreover, methanol (MeOH) is added to esterify FFAs and 10-HA, producing Fatty-Acid-Methyl-Esters or FAME and 10-Hydroxyl-Stearic-Acid-Methyl-Ester (10-HAME) respectively. Sulfuric acid is used to speed up and amplify the yield of the saponification process. After the reaction, ethyl acetate is added again to improve mixing of the organic phase. Due to high temperatures from the previous hydrogenation, vapor compounds are detected in the streams, increasing the need to remove those compounds utilizing a flash chamber. The organic phase is separated from the water phase using a liquid-liquid separator. Distillation stage takes part employing a 3-column distillation system. The central principle of the distillation process is to separate four compounds. The first, separates EtOAc and Methanol from FAME and 10-HAME. The other two, distil EtOAc and FAME respectively, resulting in four different streams. EtOAc is commonly used in different stages of the process for mixing purposes, so it is recycled. Methanol is retrieved for needs of the esterification process, while FAME (biodiesel) is consumed to power the biorefinery plant with electrical and thermal energy. The stream containing the key component 10-HAME, is then ready to proceed to the last stage of the chemical process (polymerization), after removing small amounts of admixtures utilizing a separator, to enhance the performance of the last operation. High temperatures and neutral environment (N_2) are the requirements to achieve the wanted polymerized product. Lastly, a distillation column is embedded in the system after the polymerization to recycle the unreacted monomer. The main stages of the whole chemical process are summarized in *Figure 1.9*

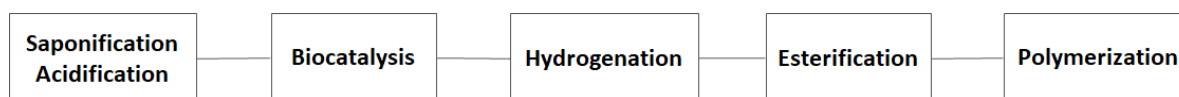


Figure 1.9: Stages of the biorefinery plant

1.7.2 Process Modelling

The bio-catalysis step was first processed based on the experimental data retrieved from a laboratory scale perspective. However, a perplexed kinetic analysis of the biomass growth needed to be conducted to examine the overall results. The kinetic tools of Aspen Plus and enzymatic models were employed to describe the incubated engineered strains of *E. Coli*. The scope was to achieve an

extended kinetic equation based on the Monod kinetic model, regarding the biomass growth, in terms of each condition examined. Enzyme growth crucially depends on the temperature, it can either enhance the growth of the biomass or it can sharply decrease the growth after a certain degree. Oxygen inhibition also plays a major role in enzyme growth increasing or decreasing the growth biomass at certain concentrations. Each of the previous conditions are examined separately regarding the growth impact. However, the results are interpolated in the extended Monod kinetic model to estimate a more integrated kinetic approach. The process modeling of bio-catalysis step was conducted in a two-way reaction system. Glucose transforms into an imaginary enzyme, for simulation purposes, via Monod kinetic approximation. Then, the produced enzyme catalyzes and converts the FFAs (second step) retrieving 10-HAs, by implementing a Michaelis-Menten (M-M) kinetic approach [6-8].

The kinetic equations are illustrated below:

$$\text{Growth:} \quad r_C = k^{cell} \cdot \frac{C_C \cdot C_S}{C_S + C_M^{Mon}} \Leftrightarrow \frac{dC_R}{dt} = k^{cell} \cdot \frac{C_C \cdot C_S}{C_S + C_M^{Mon}} \cdot \frac{C_R - C_{R0}}{C_C - C_{C0}} \quad (1.1)$$

$$\text{Temperature:} \quad r_C = r_C^{max} \cdot \frac{T_{max} - T}{T_{max} - T_{opt}} \cdot \left(\frac{T}{T_{opt}} \right)^{\frac{T_{opt}}{T_{max} - T_{opt}}} \quad (1.2)$$

$$\text{Oxygen inhibition:} \quad k_{obs} = k^{cell} \cdot \left(1 - \frac{C_{O_2}}{C_{O_2}^*} \right)^n \quad (1.3)$$

$$\text{Enzymatic conversion:} \quad r_{10HA} = k^{enz} \cdot \frac{C_{EO} \cdot C_{FFA}}{C_{FFA} + C_M^{enz}} \quad (1.4)$$

where C_i and C_{i0} are the concentrations of component i at the end of each batch experiment and the beginning, respectively; $C_{O_2}^*$ refers to the limiting concentration of inhibition; r_C defines the reaction rate of cells growth; k is the maximum growth rate; C_M refers to the Monod constant concentration, identifying produced cells when in $\frac{1}{2}$ of maximum reaction speed; k_{obs} the observed growth rate; n the exponential factor of inhibition; and T_{max} , T_{opt} and T the maximum, the optimum and the actual temperatures in cultivation medium. The indexes C, S, R and O_2 account for Cells, Substrate (glucose), Product (enzymes) and Oxygen components that participate and affect the bio-catalysis system. The conducted kinetic analysis aims to estimate the optimal conditions for the maximum growth of E. Coli bacteria, resulting in enhanced yields.

1.7.3 Sensitivity Analysis

Sensitivity analysis in a constructed process flow diagram is a methodology in which a number of variables are changed to evaluate the impact of these changes to target variables. Sensitivity analysis can utterly change the perspective of a chemical process, by altering conditions seeking for the

optimal results. In this particular biorefining plant, a sensitivity analysis was conducted in order to generate results about the bio-catalysis step; proving that the optimal result can be obtained by combining knowledge of different fields. Utilizing sensitivity analysis tool of Aspen Plus, enzyme production was observed by altering the concentration of glucose. Another analysis was conducted seeking the perfect temperature for the optimal enzyme production. Finally, oleic and linoleic acid flowrates were examined to improve the performance of bio-catalysis part, by increasing the 10-HAs production.

1.7.4 Energy Integration

Energy integration (EI) intends to minimize the need for excessive thermal and cooling energy usage; thus, it insists on seeking a way to coordinate and utilize the already existing energy that flows out of the process system. Installing heat exchangers provides the system with minimum energy needed to provide energy sustainability to a chemical process. Energy integration requires the thermal data of all the process streams extracted by the simulation process flowsheet. Energy integration has been based on the principles of Pinch analysis and the recently published biorefinery integration models of Pyrgakis and Kokossis, 2019 [9]. The model investigates the potential savings from heat integration of hot with cold streams generating energy savings for cooling and heating of each stream, respectively. The model is based on a heat transshipment modelling approach, where the heat duties of all involved streams are unfolded across the operating temperature intervals of all streams. Thus, available heat from hot streams is valorised for heating cold streams; thus, generating savings for both types of required steam and cooling utilities. To elaborate, pinch analysis is a developed method seeking energy recovery chances of an industrial site, where hot streams are utilized to heat up cold streams and cold streams are employed to cool down hot streams. Regarding a thermal system, pinch analysis is characterised by three key steps. At start, the thermal data (Temperature and Enthalpy) of hot and cold streams of all the unit operations has to be defined. Afterwards, the hot and cold composite curves of the process have to be calculated, while identifying the pinch point location, where the minimum energy is required. Eventually, the design of the heat exchange network (synthesis) has to be employed to lead to an integrated system, using the least required energy [37].

1.7.5 Life Cycle Analysis

In addition, Life Cycle Assessment (LCA) refers to a methodology in which environmental impact is estimated in a chemical process in an industrial scale when processing a product. For the stages of LCA to be completed, a summary of all the components participating in the whole chemical process need to be acknowledged. To be more specific, the amounts of every single chemical compound utilized or produced have to be considered, to examine the potential threat to the environment. Besides, the total energy of the input and output streams must be included to consequently evaluate possible environmental impacts. A Life Cycle Assessment was conducted exploiting SimaPro to estimate the mid- and end- point indicators by producing the biopolymer based on the compounds used and produced by the whole bio-catalytic process (input and output flows). Concerning the environmental indicators, the Ecoinvent databases were utilized, while the ReCiPe methods were followed for the calculations of the LCA approach. Both energy integration and LCA results will be analysed in the upcoming Chapter.

1.7.6 Techno-economic Analysis

Techno-economic Analysis or Technoeconomic Assessment (TEA) is a method utilized by numerous industries including biorefineries, traditional refineries and in general chemical processes. The intention of such an assessment is to evaluate and analyze the financial performance of a completed process; illustrating economic indicators to estimate the financial sustainability of a designed process. Creating a flawless process flowsheet biorefinery plant is pointless if the undertaking is not sustainable economically. The feasibility of the plant was estimated employing Aspen Process Economic Analyzer (APEA) and certain literature shortcut cost models, which will be analyzed thoroughly in the upcoming chapter, to evaluate missing parameters to generate an overall outcome. The target of Techno-Economic Analysis (TEA) is to calculate the CAPEX (Capital Expenditure) and OPEX (Operating Expenses) to therefore estimate economic sustainability of the biorefinery plant.

2 RESULTS OF COMPUTATIONAL ANALYSIS

2.1 BIO-CATALYSIS DESIGNING

The bio-catalysis step is processed via a two-stage reaction system. The first utilizes a good amount of glucose reacting with NO_2 and H_2O to create an imaginary enzyme $\text{C}_x\text{H}_y\text{N}_z\text{O}_w$. The enzyme that was produced was C_3HNO that would later be utilized to catalyze the after-saponification/acidification stream, saturated with FFAs. The results of the first bio-catalysis reactor are displayed in the below *Table 2.1*.

Table 2.1: Outlet/inlet streams of the first bio-catalysis

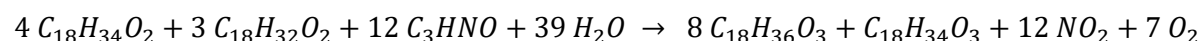
Compounds	Streams	
	GLUCOSE (kg/h)	INLET2 (kg/h)
Glucose	2100	1438.28
NO_2	1400	1062.04
H_2O	5000	4933.83
Enzyme	0	492.53
H_2	0	44.43
O_2	0	528.89

The chemical reaction that occurred in the enzyme production reactor and it is implemented into the simulation program is illustrated below:



Where $\text{C}_6\text{H}_{12}\text{O}_6$ is the molecular formula of glucose and C_3HNO is the created enzyme. The simulation considering the kinetics of the enzymatic production by glucose followed the principles of Monod kinetic equations.

The catalytic chemical reaction that followed in the next bio-catalysis phase, ending in the reacted FFA stream obtaining the hydroxyl group (OH^-) in the 10th carbon of the acids is also depicted in the equation below.



Where, $\text{C}_{18}\text{H}_{34}\text{O}_2$, $\text{C}_{18}\text{H}_{32}\text{O}_2$, $\text{C}_{18}\text{H}_{36}\text{O}_3$ and $\text{C}_{18}\text{H}_{34}\text{O}_3$ are the chemical formulas of oleic, linoleic, 10-HA and 2.10-HA (10-HA with a double bond between $\text{C}_{12} = \text{C}_{13}$) respectively. The produced 2.10-HA is experimentally estimated to be roughly 10-20% of the total 10-HAs. The kinetic principles were adjusted in the simulation engine utilizing Michaelis-Menten kinetics, that were implemented into the simulation process.

Table 2.2: Outlet/Inlet streams of the second bio-catalysis

Compounds	Streams		
	S53 (kg/h)	INLET2 (kg/h)	S10 (kg/h)
OLEIC	1445.651074	0	0.26484274
LINOLEIC	589.8311481	0	0.10805685
PALMITIC	194.2561149	0	194.256115
STEARIC	0	0	119.919913
Glucose	0	1438.28	1438.28391
NO ₂	0	1062.04	47801.5896
H ₂ O	0	4933.83	0.1419365
Enzyme	0	492.53	0.0902305
H ₂	0	44.43	44.43
O ₂	0	528.89	528.89
10HYDRA	0	0	1808.154
2.HYDRA	0	0	221.8

The stream INLET2 mainly consists of the previously produced enzyme, while stream S53 contains substantial amounts of FFAs and unreacted amounts of previously used reactants in saponification/acidification steps. The main components that participate in BIOCAT2 block are summarized in the above *Table 2.2*. The reactants oleic and linoleic acid are going through a catalyzed reaction, resulting in the key components 10-HAs. It is estimated via the Aspen process simulation that about 1446 kg of oleic acid and 589 kg of linoleic acid (a total of 2.035 kg) produce about 2000 kg of 10-HAs. The upcoming separator is used as a membrane to remove admixtures such as the enzyme that blocked the following processes due to failed simulations of the program. *Figure 2.1* illustrates the process flow sheeting of the bio-catalysis stage, in association with the streams that participate.

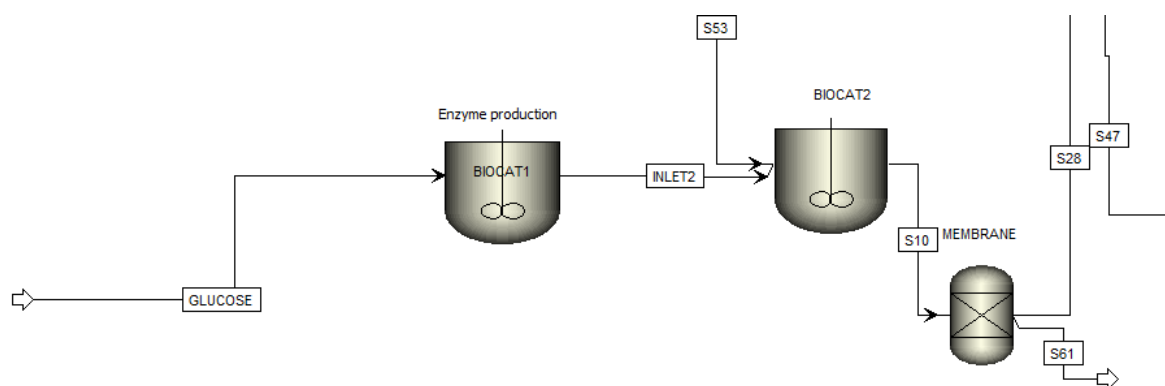


Figure 2.1: Two-stage bio-catalysis reactors

Both bioreactors operate at a constant temperature of 37 °C, under atmospheric pressure (1 atm) to ensure optimal results with the lower energy cost.

2.2 KINETIC MODELS OF BIO-CATALYSIS

For the bio-catalysis modelling to be precise, a detailed modification of Monod's kinetic model is necessary. The first bio-catalysis stage is expressed by the Monod kinetic model, while the enzymatic conversion of FFAs is described by Michaelis-Menten kinetic approach. The novel chemistry creates the need for further kinetic search to establish a more integrated result. Experimental data originated from literature knowledge were combined with the tools from Aspen Plus simulation engine to build kinetic equations and estimate and institute the kinetic results presented in the following paragraphs.

2.2.1 Bio-catalysis producing the enzyme

For manufacturing the desired enzyme, E. Coli cells are fermented, employing glucose as a chemical substrate for biomass growth. In the chemical bioreactor, glucose reacts with NO_2 and water to result in the constructed imaginary enzyme for simulation purposes as depicted on *Table 2.1*. Monod kinetic equation was implemented to further investigate the kinetic results of the bio-catalysis. Numerous reaction conditions play a major role in the growth of biomass and could either increase or sharply decrease the yield of the bio-catalysis. Certain conditions were examined for the impact they can impose on the specific bio-catalysis reaction. For instance, the temperature in which E. Coli cells are fermented is extremely crucial, as the range in which E. Coli cells can flourish is tiny and should be carefully regulated. Moreover, the amount of oxygen needed for a fermentation process should be carefully controlled, since oxygen occasionally limits/decelerates the growth of biomass (product poisoning). To combine the different approaches to estimate the limitations and results of the overall kinetic analysis, an extended Monod kinetic model should be constructed. For this cause, it is necessary to separate the bio-catalysis, in two different reactors, for simulation engine's purposes.

Monod's kinetic model is presented in Equation (2.2).

$$r_c = \frac{kC_A C_C}{C_A + C_M} \quad (2.2)$$

Where, r_c , describes the growth of E. Coli cells, k , indicates a Monod's constant related with the speed, C_A , C_C , define the concentration of both the substrate (glucose) and the cell's concentration (E. Coli) respectively, while C_M refers to as half saturation constant or affinity constant.

The pathway followed to construct the extended kinetic model is perplexed and presented in detail below.

In order to evolve the Monod's mathematical equation, it is obligatory to define a simple stoichiometric reaction, as presented below in Equation (2.3).



Based on the literature that was followed (Octave Levenspiel, 2011, chapters 27-29) an instantaneous fractional yield is depicted below utilizing a shorthand notation.

$$\boxed{\frac{C}{A}} = \varphi \left(\frac{C}{A} \right) = \frac{d(C_{formed})}{d(A_{used})} \quad (2.4)$$

$$\boxed{\frac{R}{A}} = \varphi \left(\frac{R}{A} \right) = \frac{d(R_{formed})}{d(A_{used})} \quad (2.5)$$

$$\boxed{\frac{R}{C}} = \varphi \left(\frac{R}{C} \right) = \frac{d(R_{formed})}{d(C_{used})} \quad (2.6)$$

In this case, the following expressions are extracted.

$$\boxed{\frac{R}{A}} = \boxed{\frac{R}{C}} + \boxed{\frac{C}{A}} \quad (2.7)$$

$$\boxed{\frac{A}{C}} = 1 / \boxed{\frac{C}{A}} \quad (2.8)$$

And the rate of the bacteria/cell or enzyme's growth is expressed as follows.

$$r_C = (-r_A) \left(\boxed{\frac{C}{A}} \right) \quad (2.9)$$

$$r_R = (-r_A) \left(\boxed{\frac{R}{A}} \right) \quad (2.10)$$

$$r_R = (-r_A) \left(\boxed{\frac{R}{C}} \right) \quad (2.11)$$

When working with instantaneous fractional yields, stoichiometry analysis tends to be inaccessible, when compositions change. Reasonably, it is considered that all the φ values are constant. Therefore, it can be assumed, utilizing Equations (2.4)-(2.6) that:

$$C_C - C_{C0} = \boxed{\frac{C}{A}} (C_{A0} - C_A) \quad (2.12)$$

$$C_R - C_{R0} = \boxed{\frac{R}{A}} (C_{A0} - C_A) \quad (2.13)$$

$$C_R - C_{R0} = \left[\frac{R}{C} \right] (C_C - C_{C0}) \quad (2.14)$$

All the above mathematical equations are illustrating the pathway followed to alter the Monod's approach. Monod kinetic equation calculates the growth of E. Coli cells $r_C \Rightarrow \frac{dC_{cells}}{dt} \Rightarrow \left[\frac{C}{A} \right]$, however, the need for this thesis is to extrapolate the kinetic evaluations regarding the enzyme production utilizing the E. Coli strains. Therefore, concerning Monod's kinetic equation, it is necessary to convert the mathematical equations. Taking advantage of Equations (2.6), (2.7), (2.11) and (2.14), Monod's equation formation is as follows.

$$dC_R = (-r_A) \left[\frac{R}{C} \right] \quad (2.15)$$

Equation (2.15) ends up in Equation (1.1): $\frac{dC_R}{dt} = k^{cell} \cdot \frac{C_C \cdot C_S}{C_S + C_M^{Mon}} \cdot \frac{C_R - C_{R0}}{C_C - C_{C0}}$ depicted on the previous chapter, showing and giving the advantage to calculate the kinetic growth of the produced enzyme over time.

There is a huge need for calculating Monod's equation constants, regarding the specific bio-catalysis, to extract the kinetic estimations, so additionally, an extended analysis was conducted. After various mathematical transformations, based on (O. Levenspiel, 2011, chapter 29) literature, as well as laboratory experiments, an equation was extracted for the calculation of Monod's constant values.

$$\frac{1}{C_A} = \frac{k}{C_M} \tau_m + \frac{1}{C_M} \quad (2.16)$$

Where τ_m presents the mixed flow performance equation (time).

The form of the equation is the general equation of a straight line ($y = ax + b$), where a is the gradient (slope) and $y = b$ is the value where the straight line intercepts the y-axis. Employing literature data for utilizing glucose as a substrate for E. Coli bacteria fermentation, experimental data were collected [7]. The below table indicates the simple calculations made to further draw the experimental straight line.

Table 2.3: Glucose concentration (mmol/l) in association with the time (h)

Glucose (mmol/l)	Time (h)	1/Ca	Ca (g/ml)
81	0	0.012346	14592.96
81	2	0.012346	14592.96
80	5	0.012500	14412.80
79	6	0.012658	14232.64
72	6.5	0.013889	12971.52
69	7	0.014493	12431.04
63	7.5	0.015873	11350.08
60	8	0.016667	10809.60
58	8.5	0.017241	10449.28

57	9	0.017544	10269.12
55	10	0.018182	9908.80
53	12	0.018868	9548.48
51	14	0.019608	9188.16
48	24	0.020833	8647.68
46	30	0.021739	8287.36
43	36	0.023256	7746.88
39	48	0.025641	7026.24

Utilizing the data of *Table 2.3*, the below graph is created that assists in calculating the unknown constants of the Monod's equation.

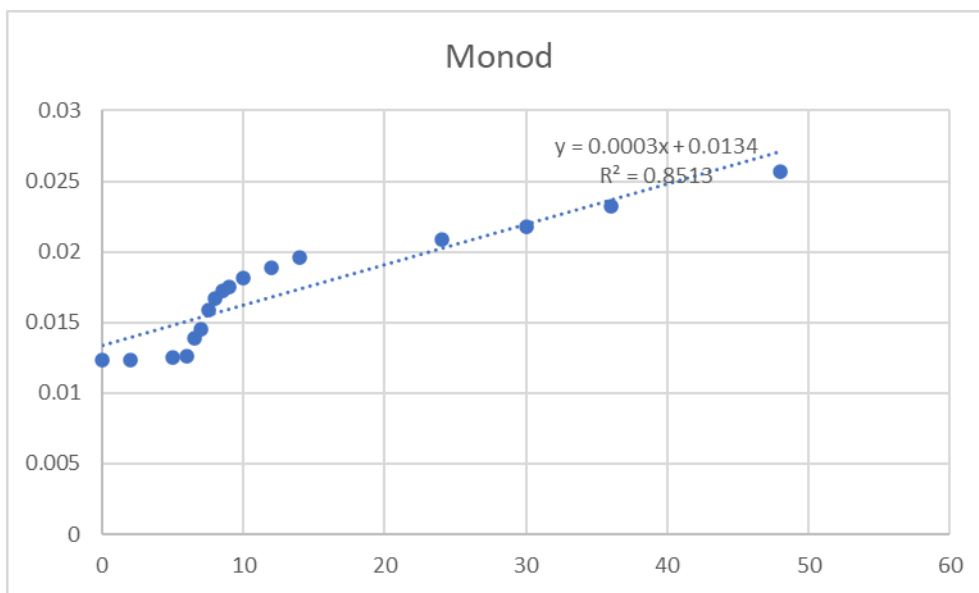


Figure 2.2: Graph to calculate Monod's constant values

The experimental data, as shown in *Figure 2.2*, approach a straight line formation. R^2 (Coefficient of Determination), which stands for a statistical measure that indicates the percentage of variance in a dependent variable, is representing relatively trusted results. From the above graph, results were obtained regarding the slope of the straight line, which stands for $slope = \frac{k}{C_M}$. Therefore, $k = 0.022388 \text{ 1/h}$ and $C_M = 74.62687 \text{ mmol/l}$.

A more comprehensive analysis on the kinetic models can be found on [Octave's Levenspiel 2011, chapters 28,29].

All the above calculations can be utilized to estimate and evaluate O_2 limitation impact of poisoning the product, as well as the impact of the temperature during the fermentation of E. Coli, and in general any fermentation/incubation of cells.

Concerning O_2 concentration limitation, literature data provided a mathematical expression, in which product poisoning decreases the growth of microorganisms such as bacteria or cells. This expression can be adjusted to the traditional Monod's equation, to assist in calculating E. Coli bacteria growth

under the influence and presence of oxygen. Therefore, the concentration of oxygen that imposes an impact on the growth of bacteria is represented through the following expression, also referred to in Chapter 1.

Oxygen Inhibition:
$$k_{obs} = k^{cell} \cdot \left(1 - \frac{C_{O_2}}{C_{O_2}^*}\right)^n \quad (1.3)$$

Where the limiting oxygen's concentration of inhibition ($C_{O_2}^* = 0.12 \frac{mg}{L}$ or $0.0075 \frac{mmol}{L}$) is calculated from experimental data. Based on the previously conducted analysis for the growth of E. Coli cells, combined with the knowledge of the constant value of oxygen's inhibition limit, a graph was able to be created showing the O₂ concentration impact when it comes to fermenting E. Coli cells [30]. The below *Table 2.4* summarizes the collected and calculated data concerning O₂ impact to a fermentation process involving E. Coli, regarding the overall biomass growth.

Table 2.4: Kinetic growth rate of E. Coli with respect to oxygen's concentration

dC/dt (mM/h)	C _{O₂} (mmol/l)
0.011652441	0.323280592
0.011652441	0.323280592
0.011583012	0.323302172
0.011512679	0.323324033
0.010993485	0.323485412
0.010755482	0.323559389
0.010248346	0.32371702
0.009977827	0.323801104
0.009790682	0.323859274
0.009694977	0.323889021
0.009499136	0.323949893
0.009297158	0.324012673

The above kinetic results indicate that oxygen imposes a great threat when fermenting E. Coli cells (product poisoning), so careful management is required; thus, oxygen regulation during the bio-catalysis process is mandatory. The above data are summarized in *Figure 2.3* depicting O₂ impact in the bio-catalysis process.

It should be noted that all the collected data was specifically based on E. Coli strains, to obtain a more realistic and trusted perception. From *Figure 2.3*, it is evident that the higher the concentration of oxygen in the bio-catalysis, the lower the growth of E. Coli cells; concluding that oxygen decreases the overall kinetic growth.

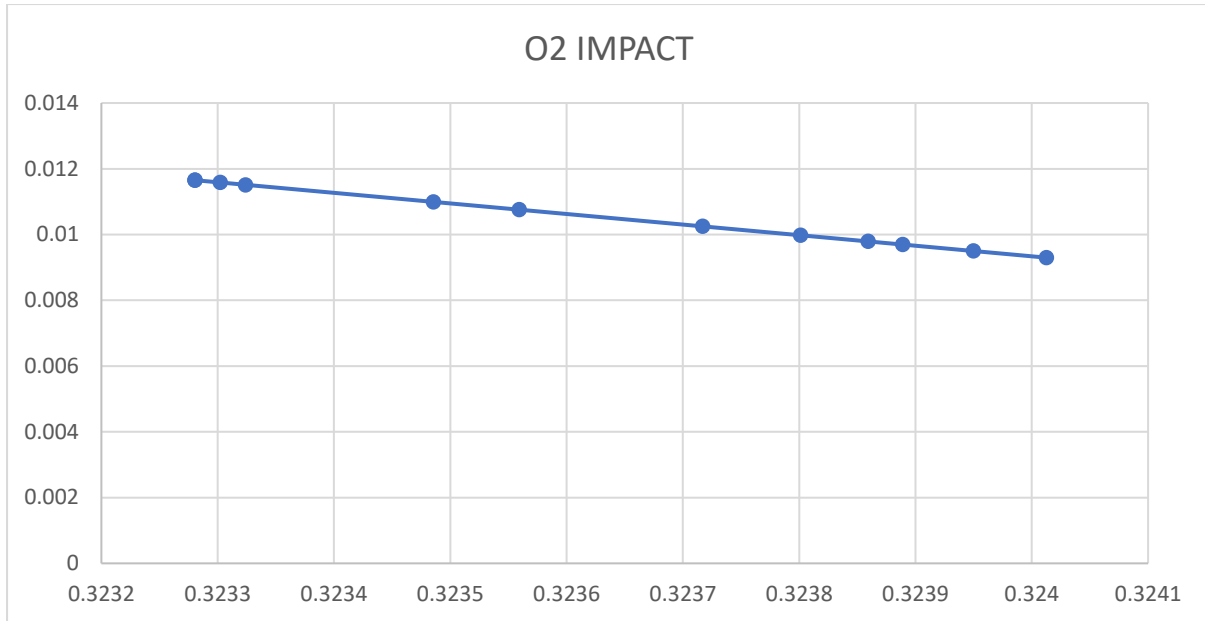


Figure 2.3: Kinetic growth of E. Coli strains regarding the concentration of O₂

Continuing with kinetic growth of E. Coli cells behavior concerning temperature changes. Temperature is one of the most crucial conditions in respect of chemical reactions, especially when reactions include microorganisms. E. Coli cells flourish in a slight temperature range; so, controlling and understanding the impact of temperature is a key factor in bio-catalysis research. Temperature's effect on microbial growth is represented in the below Equation (1.2), also included in Chapter 1.

Temperature:

$$r_C = r_C^{max} \cdot \frac{T_{max} - T}{T_{max} - T_{opt}} \cdot \left(\frac{T}{T_{opt}} \right)^{\frac{T_{opt}}{T_{max} - T_{opt}}} \quad (1.2)$$

The above kinetic expression is utilized to include temperature effect on the general model of the Monod kinetic equation. Collecting literature data regarding temperature impact on fermentation of E. Coli cells can lead to a deep understanding of the bio-catalysis temperature influence. Maximum and optimum temperature are constants drained from literature that examined the growth of E. Coli cells regarding temperature (315.2 K and 311.9 K respectively); maximum relative growth rate is also a known quantity (7.2 1/day). Equation (1.2) is also extracted via experimental procedures, indicating highly accurate estimations regarding microorganisms in general and of course E. Coli [31-33]. In the below *Table 2.5*, temperature data is summarized to calculate the overall temperature impact on the kinetic growth of the bacteria, as it will be later used to construct the extended Monod equation, that will be analyzed thoroughly in the upcoming chapters.

Table 2.5: Temperature's impact on kinetic growth

T(K)	R(T)
275.7	0.000744
280	0.002862
285	0.01308
290	0.05648
295	0.227788
300	0.83929
305	2.686293
310	6.368085
311.9	7.2
315	1.11124
315.2	0
316	-5.99751

Employing the above temperature data, a graph can be extracted to depict the huge significance of temperature regarding the kinetic growth of E. Coli. *Figure 2.4* clarifies the above analysis, illustrating the magnitude of such a kinetic analysis.

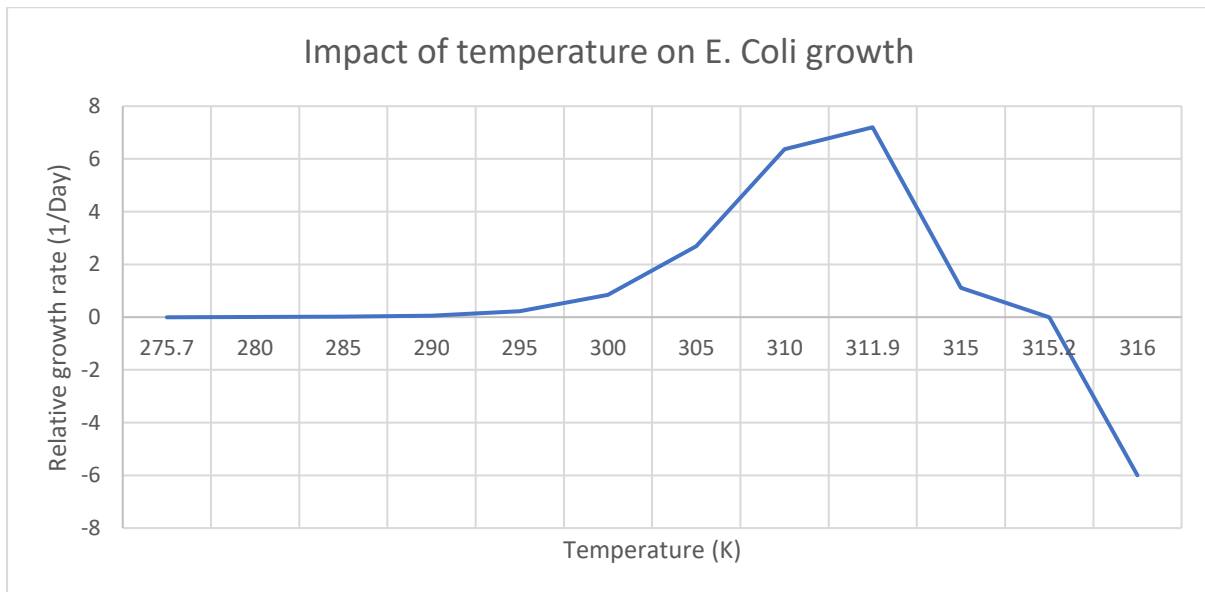
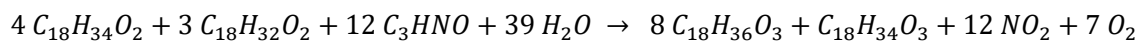


Figure 2.4: Schematization of kinetic growth regarding temperature

The above graph clearly shows that bio-catalysis has an optimum temperature around 311.9 K (or 38.73 °C) that provides the bio-catalysis with higher yields. It should also be noted that after a certain temperature range the growth rate sharply decreases, indicating that bio-catalysis should be carefully managed.

2.2.2 Enzymatic conversion of FFAs

For manufacturing the kinetic model for the enzymatic conversion of FFAs into the key fatty acids (10-HAs) a separate bioreactor was utilized to further investigate the kinetic results of the bioreaction. To be more specific, the imaginary enzyme catalyzes and enhances the selectivity of the bioreaction to produce the desired products. The chemical reaction that occurred and utilized for the simulation engine is presented below and is also displayed at the start of Chapter 2.



For that cause, Michaelis-Menten (M-M) kinetic model was implemented, to describe and explain the kinetic expressions followed by the enzymatic conversion of FFAs. M-M kinetic model is expressed in Equation (2.17)

$$-r_A = r_R = \frac{k(C_{E_0} C_A)}{C_M + C_A} \quad (2.17)$$

Where, $-r_A$ describes the rate of reduction of the substrate, while r_R describes the rate of production of the key products. Also, k describes a kinetic M-M kinetic constant, while C_{E_0} and C_A depict the concentration of the enzyme and the concentration of the substrate (FFAs) respectively, while C_M refers to a M-M constant value. To elaborate, the goal is to calculate the missing parameters of the Equation (2.17). So, accordingly, literature data was collected including FFA reduction during an enzymatic bio-catalysis [27]. Based on [Octave Levenspiel 2011, chapter 27], the goal is to create Eadie Diagram to calculate C_M and k of the enzyme or k^{enz} . Eadie Diagram is schematized by collecting data of the rate of the reduction of the substrate ($-r_A$) in correlation with $-\frac{r_A}{C_A}$. For this cause the below *Table 2.6* was created to calculate these values on a specific time.

Table 2.6: Depiction of calculations for the drawing of Eadie Diagram utilizing literature data

% of FFAs	FFA (mol)	Time (min)	mol/min	C(FFA) mol/L	(-r(A))	(-r(A))/Ca
100	8400.204	1		1.7049	0	0
70	5880.143	3	1960.0476	1.1934	0.1705	0.1429
43	3612.088	10	361.2088	0.7331	0.0972	0.1326
24	2016.049	30	67.2016	0.4092	0.0432	0.1056
20	1680.041	60	28.0007	0.3410	0.0227	0.0667
15	1260.031	120	10.5003	0.2557	0.0121	0.0472
10	840.0204	240	3.5001	0.1705	0.0064	0.0375
8	672.0163	420	1.6000	0.1364	0.0037	0.0274

Being aware of the reduction of FFAs under an enzymatic bio-catalysis throughout time and the amount of FFAs in the bioreactor, calculating the concentration of FFAs is easily concluded. Therefore, the prerequisites of the Eadie Diagram are calculated. The next step is to create the graph in order to be able to determine these constants utilizing the slope and the interception of the x-axis of the

schematized line. Ultimately, by utilizing the data retrieved through the above *Table 2.6*, the Eadie Diagram is drawn and depicted in *Figure 2.5*.

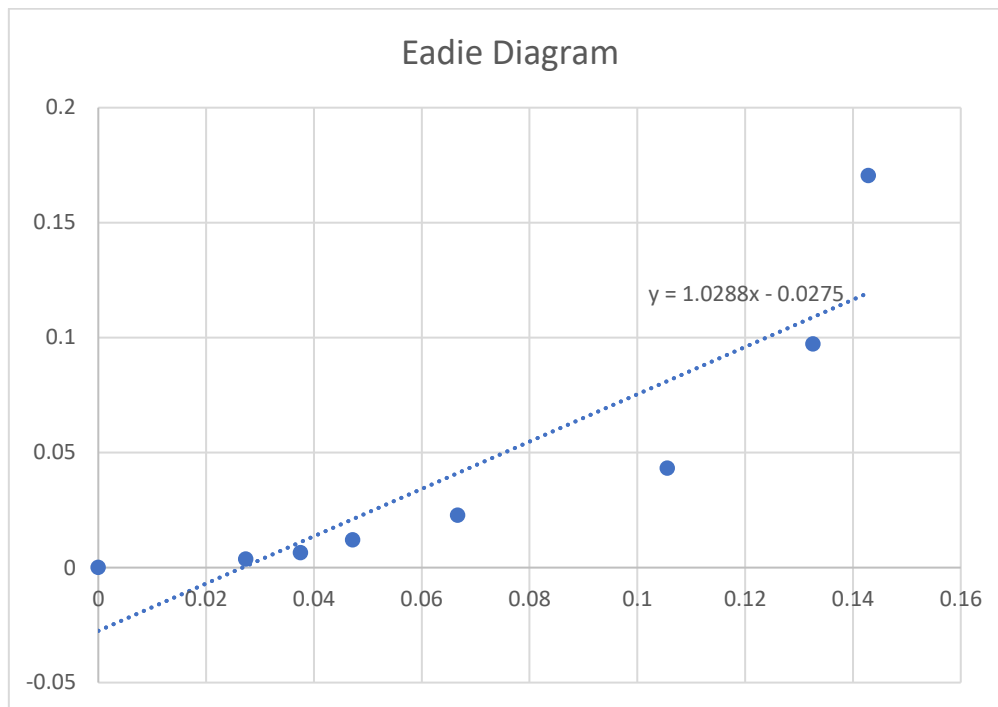


Figure 2.5: Schematization of Eadie Diagram to compute M-M constants

This kinetic model approach resulted in calculating $k^{enz} = 1.0288 \text{ mol/L}$ derived from the slope of the experimental line. C_M constant was also determined as the point in which the experimental line intercepts the x-axis. Specifically, this point is the value of $\frac{C_M}{k^{enz}}$, so roughly $C_M = 0.025 \text{ mol/L}$.

After calculating the kinetic quantities for a better understanding of the bio-catalysis reaction, both kinetic models (Monod's and M-M) have to get inserted into the Aspen Plus simulation process to consequently acquire the desired results. The first step is to build the reactions in Aspen Plus in the two separate bioreactors. Both reaction set-ups follow the generalized Langmuir-Hinshelwood-Hougen-Watson (LHHW) model. Aspen Plus provides a LHHW input kinetic sheet/expression to specify kinetic data for rate-controlled reactions to calculate the reaction rate. Depending on Aspen Plus build-in reaction set-ups, the general LHHW expression is presented in Equation (2.18).

$$r = \frac{(\text{kinetic factor})(\text{driving force})}{(\text{adsorption term})} \quad (2.18)$$

Where, kinetic factor, driving force and adsorption term are illustrated in the below *Figure 2.6*.

$$\begin{aligned}
\text{Kinetic factor} &= k(T/T_o)^n e^{-(E/R)[1/T-1/T_o]} \\
\text{Driving force expression} &= k_1 \prod_{i=1}^N C_i^{\alpha_i} - k_2 \prod_{j=1}^N C_j^{\beta_j} \\
\text{Adsorption term} &= \left[\sum_{i=1}^M K_i \left(\prod_{j=1}^N C_j^{\nu_j} \right) \right]^m
\end{aligned}$$

Figure 2.6: Aspen Plus kinetic equations based on the general LHHW form

In consequence, the already built kinetic equations must be altered using mathematics to get into the desired expression “shape”. Utilizing the Equations (1.1, 1.2, 1.3, 2.2 and 2.15) the extended kinetic model of Monod is shown in Equation 2.19.

$$dC_R = - \frac{k \frac{C_A C_C}{C_A + C_M} k_{obs} \left(1 - \frac{C_R}{C_R^*}\right) R_{max} (T_{max} - T)}{T_{max} - T_{opt}} \left(\frac{T}{T_{opt}}\right)^{\frac{T_{opt}}{T_{max} - T_{opt}}} (C_{A_0} - C_A) \quad (2.19)$$

With the use of different mathematical approaches to alter the above Equation (2.19), to resemble Equation (2.18), it was feasible to create a kinetic model suitable for the generalized LHHW form. Equation (2.19) was modified and led to the below mathematical expressions regarding kinetic factor, driving force and adsorption term (Equations 2.20-2.22).

$$\text{Kinetic factor} = \frac{k R_{max} (C_A - C_{A_0}) (T_{max} - T)}{T_{max} - T_{opt}} \left(\frac{T}{T_{opt}}\right)^{\frac{T_{opt}}{T_{max} - T_{opt}}} \quad (2.20)$$

$$\text{Driving force} = -k_{obs} (C_R^* C_A C_C + k_{obs} C_R C_R^*) \quad (2.21)$$

$$\text{Adsorption term} = (C_A + C_M) C_R^* \quad (2.22)$$

The same approach was followed when seeking kinetic reaction LHHW forms for the conversion of FFAs through the M-M kinetic model. Michaelis-Menten kinetic model was undemanding when attempting to create the kinetic expressions of Equation (2.18) because mathematical transformations were mainly unnecessary. The M-M kinetic model, as shown previously in Equation (1.4) is prepared to seek for the desired LHHW expressions. In consequence, the needed forms are depicted in the below Equations (2.23-2.25).

$$\text{Kinetic factor} = k_{enz} \quad (2.23)$$

$$\text{Driving force} = C_{E_0} C_{FFA} \quad (2.24)$$

$$\text{Adsorption term} = (C_{FFA} + C_M^{Enz})^{-1} \quad (2.25)$$

All the above Equations (2.20-2.25) are utilized as kinetic input for the generalized LHHW form of Aspen Plus, to provide validity to the estimations for a more integrated overall kinetic result, both for the bio-catalysis (Monod) and the enzymatic conversion of FFAs (M-M).

2.3 UPSTREAM AND DOWNSTREAM PROCESSES

All the above data as well as the experimental data derived from laboratory experiments, were collected and examined seeking further estimations about the whole processes of the biorefinery. The intention of doing so was to evaluate the yields of all the upstream and downstream processes of this novel biochemical refinery. Scaling-up, through a process simulation engine like Aspen Plus gives the opportunity to estimate overall yields of chemical processes; thus enables the comparison of experimental (laboratory scale) with computational processing approaches (Aspen Plus) to ultimately obtain a trustworthy and more integrated process evaluation. This Chapter will illustrate the overall outcomes of all the processes that participated in the undertaking in correlation with the experimental yields derived from laboratory scale observations. It should be noted that not all the components are included in the tables because of the lack of their significance.

2.3.1 Saponification-Acidification

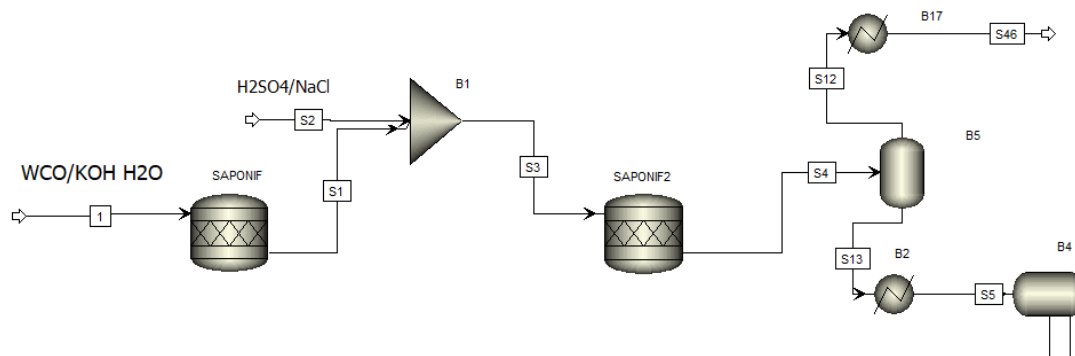


Figure 2.7: Saponification/Acidification steps in Aspen Plus flowsheet

Saponification (SAPONIF) and acidification (SAPONIF2) are two consecutive processes to primarily transform the triglycerides of WCOs into soaps and convert them into acids (FFAs). Both reactions occur implementing RSTOIC model reactors under similar conditions (80°C and ambient pressure). The opening of the project comes begins from the recycled used cooking oils (RUCO) in forms of triglycerides (TGs), where 3 tons react with a strong alkali (KOH) with the utilization of ethanol that accelerates the saponification process [25]. Afterwards, the acidification process takes place, in which the produced soaps react with a strong acid (H₂SO₄), in presence of NaCl that helps in separation, to finally produce FFAs in stream S4. Then the separation of the organic from the water phase occurs as depicted in *Figure 2.7*. The below *Table 2.7* illustrates the main quantities of the compounds interacting with in the two reactors.

Table 2.7: Saponification/Acidification process inputs and outputs

Compounds	Streams (kg/h)				
	1	S1	S2	S3	S4
TG-OLEIC	1673.8	83.7	0.0	83.7	83.7
TG-LINOL	683.1	34.2	0.0	34.2	34.2
KOH	1632.9	1136.8	0.0	1136.8	1136.8
WATER	1020.6	1020.6	17635.7	18656.3	18656.3
ETHANOL	7144.1	7144.1	0.0	7144.1	7144.1
TG-PAL	225.9	11.3	0.0	11.3	11.3
TG-STEAR	138.8	6.9	0.0	6.9	6.9
POLEATE	0.0	1726.9	0.0	1726.9	86.3
PLINOLEA	0.0	705.2	0.0	705.2	35.3
PPALMITA	0.0	234.9	0.0	234.9	11.7
PSTEREAT	0.0	143.1	0.0	143.1	7.2
GLYCEROL	0.0	271.4	0.0	271.4	271.4
NACL	0.0	0.0	4664.7	4664.7	4664.7
H2SO4	0.0	0.0	12451.1	12451.1	11627.2
KHSO4	0.0	0.0	0.0	0.0	1143.9
OLEIC	0.0	0.0	0.0	0.0	1445.7
LINOLEIC	0.0	0.0	0.0	0.0	589.8
PALMITIC	0.0	0.0	0.0	0.0	194.3
STEARIC	0.0	0.0	0.0	0.0	119.9

Compounds such POLEATE and PLINOLEA retrieved from *Table 2.7*, refer to as potassium oleate and potassium linoleate respectively, as the soaps, claimed from the saponification stage. Oleic, Linoleic, Palmitic and Stearic acids are referred to as FFAs.

2.3.2 Bio-catalysis

The below *Figure 2.8* demonstrates the bio-catalysis process, in which glucose is used as a substrate to further grow the engineered E. Coli strains, producing the imaginary enzyme (BIOCAT1) necessary for the upcoming stage of the bio-catalysis. Furthermore, the enzyme catalyses the FFAs with the assistance of various bio-enhancers like IPTG and Kanamycin in (BIOCAT2), where the key-components are produced. The upcoming membrane is implemented into the system to remove undesired components like the imaginary enzyme that causes malfunctions to the simulation engine on approaching processes. Onwards, EtOAc is utilized for mixing purposes to eventually retrieve the produced organic phase via a centrifuge and a spray dryer consecutively.

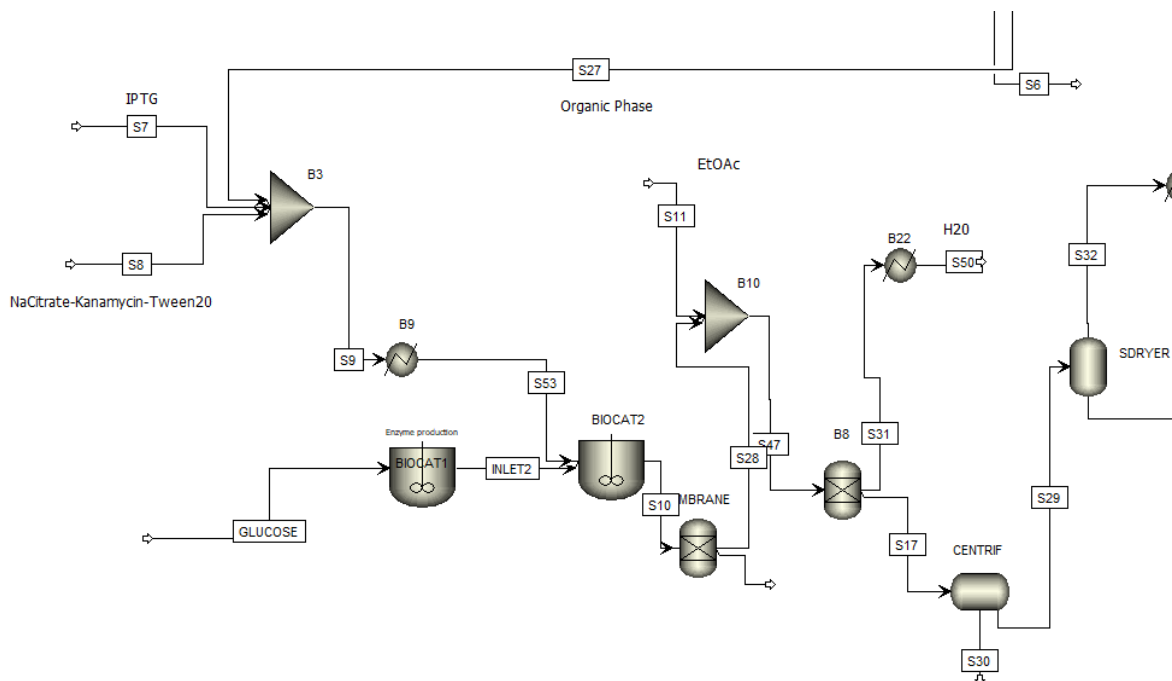


Figure 2.8: Bio-catalysis part in Aspen Plus flowsheet

The below *Table 2.8* summarizes the main components both of the (BIOCAT1) and (BIOCAT2) inlets and outlets.

Table 2.8: Inlets and outlets of the Bio-catalysis stage derived from Aspen Plus process simulation

Compounds	Streams (kg/h)			
	GLUCOSE	INLET2	S53	S10
GLUCOSE	2100	1438.284	0	1438.284
NO ₂	1400	1062.045	0	47801.59
H ₂ O	5000	4933.83	0	0.141936
ENZYME	0	492.5256	0	0.090231
H ₂	0	44.42576	0	44.43
O ₂	0	528.8897	0	528.8897
OLEIC	0	0	1445.651	0.264843

LINOLEIC	0	0	589.8311	0.108057
PALMITIC	0	0	194.2561	194.2561
STEARIC	0	0	119.9199	119.9199
10HYDRSA	0	0	0	1808.154
2.HYDRSA	0	0	0	221.8

Both bioreactors employ RCSTR model, that requires the kinetic data of the occurred reactions, under the influence of indistinguishable conditions key for the fermentation (37°C and ambient pressure).

2.3.3 Hydrogeneration

Figure 2.9 illustrates the inlets and outlets of the hydrogeneration process, where saturated along with unsaturated FFAs react with molar hydrogen to break the double carbon-carbon bonds. S33 stream consists of the main acids originated from bio-catalysis stem, while S19 stream contains an excess amount of H₂.

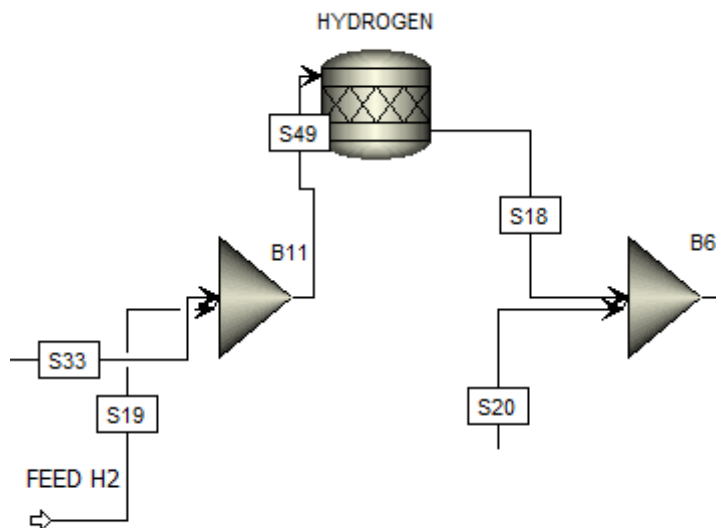


Figure 2.9: Hydrogeneration process derived from Aspen Plus flowsheet

The whole modelling was conducted implementing RSTOIC stoichiometric reactor that is based on known fractional conversions. Hydrogeneration in general demands high temperatures or a catalyst to enable the addition reaction to occur. A nickel-based catalyst is employed to decrease the required temperature of the process to 150°C in ambient pressure.

Table 2.9: Inlets and outlets of the hydrogeneration process

Compounds	Streams (kg/h)		
	S33	S19	S18
OLEIC	0.244	0	0.006
LINOLEIC	0.095	0	0.002
PALMITIC	179.278	0	179.278

STEARIC	108.785	0	109.116
10HYDRSA	1807.257	0	2016.162
2.HYDRSA	219.900	0	10.990
H2	0	22.000	44.426

The above *Table 2.9* summarizes the key results of the hydrogenation process, where 10-HA (10HYDRSA) is generated in adequate purity.

2.3.4 Esterification

The below *Figure 2.10* depicts the inlets and outlets of the esterification process. S18 is the key stream consisting of the hydrogenated FFAs retrieved from the previous process, while S20 is a new feed-stream in which new reactants like methanol are added to begin the esterification process. A strong acid (H_2SO_4) is employed as a catalyst to enhance the reaction. During the simulation process, a flash reactor (FLASH2 or B14) is utilized to remove the existing small percentages of vapors that create an issue when it comes to separating the two generated liquids. Afterwards, a liquid-liquid separator is implemented to separate the organic from the water phase using EtOAc as usual for mixing purposes, to consequently improve the separating conditions.

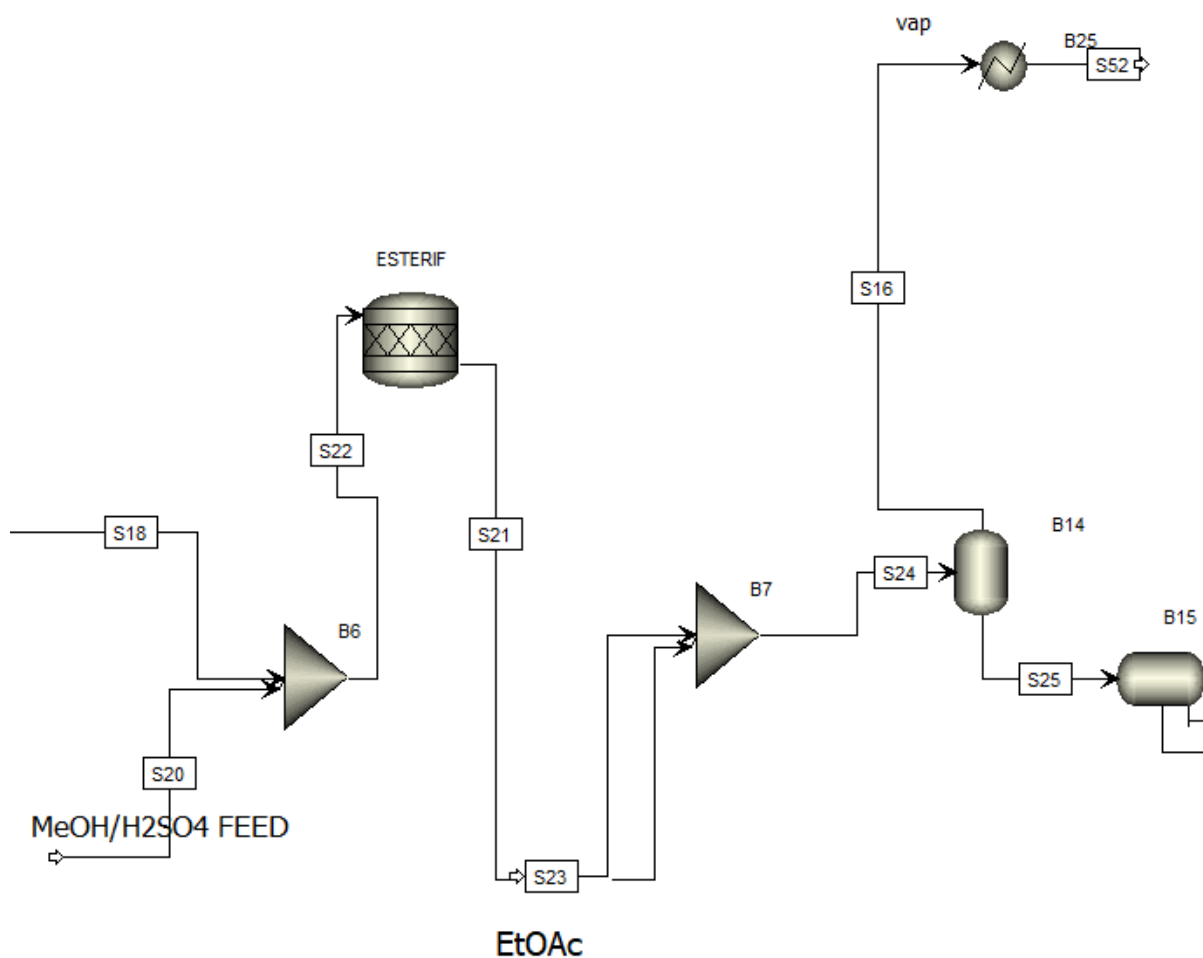


Figure 2.10: Schematization of esterification process in Aspen Plus flowsheet

The esterification process was modelled using an RSTOIC reactor based on known stoichiometric data for the process. The modelling was conducted in ambient pressure and temperature of 80°C. The below *Table 2.10* indicates the primary inlets and outlets of the esterification process in order to evaluate the upcoming results.

Table 2.10: Inlets and outlets of the esterification process retrieved from the Aspen Plus simulation engine

Compounds	Streams (kg/h)		
	S18	S20	S21
PALMITIC	179.278	0	8.964
STEARIC	109.116	0	5.456
10HYDRSA	2016.162	0	100.808
2.HYDRSA	10.990	0	10.990
MEOH	0	1765.382	585.214
H2SO4	0	1095.879	1095.879
STERFAME	0	0	103.982
PALMFAME	0	0	172.739
10HSAME	0	0	1732.640

2.3.5 Distillation

During the distillation process, three different distillation columns (DSTWU) are implemented to separate the key components of the esterification process's outlet stream. The below *Figure 2.11* schematizes the whole process flow sheeting of the distillation process, where the first distillation column (DIST1) separates the heavier components (FAME and 10-HAME) from the lighter components (Methanol and Ethyl acetate). The following distillation columns (DIST2 and DIST3) assist in isolating methanol from ethyl acetate and FAME from the key component 10-HAME. The stream containing 10-HAME (S40) undergoes a separation process to enhance the levels of purity before inserting into the polymerization reactor.

The below *Table 2.11* illustrates the main components taking part during the underlying process. It should be noted that all the distillation columns contained a condenser and a reboiler working roughly in ambient pressure.

Table 2.11: Main Inlets and outlets of the three-stage distillation process

Compounds	Streams (kg/h)				
	S26	S54	S55	S56	S42
MEOH	585.214	581.407	0	0	0
ETOAC	115.287	0	114.002	0	0
STERFAME	103.982	0	0	102.438	0
PALMFAME	172.739	0	0	170.227	0
10HSAME	1732.640	0	0	0	1729.282

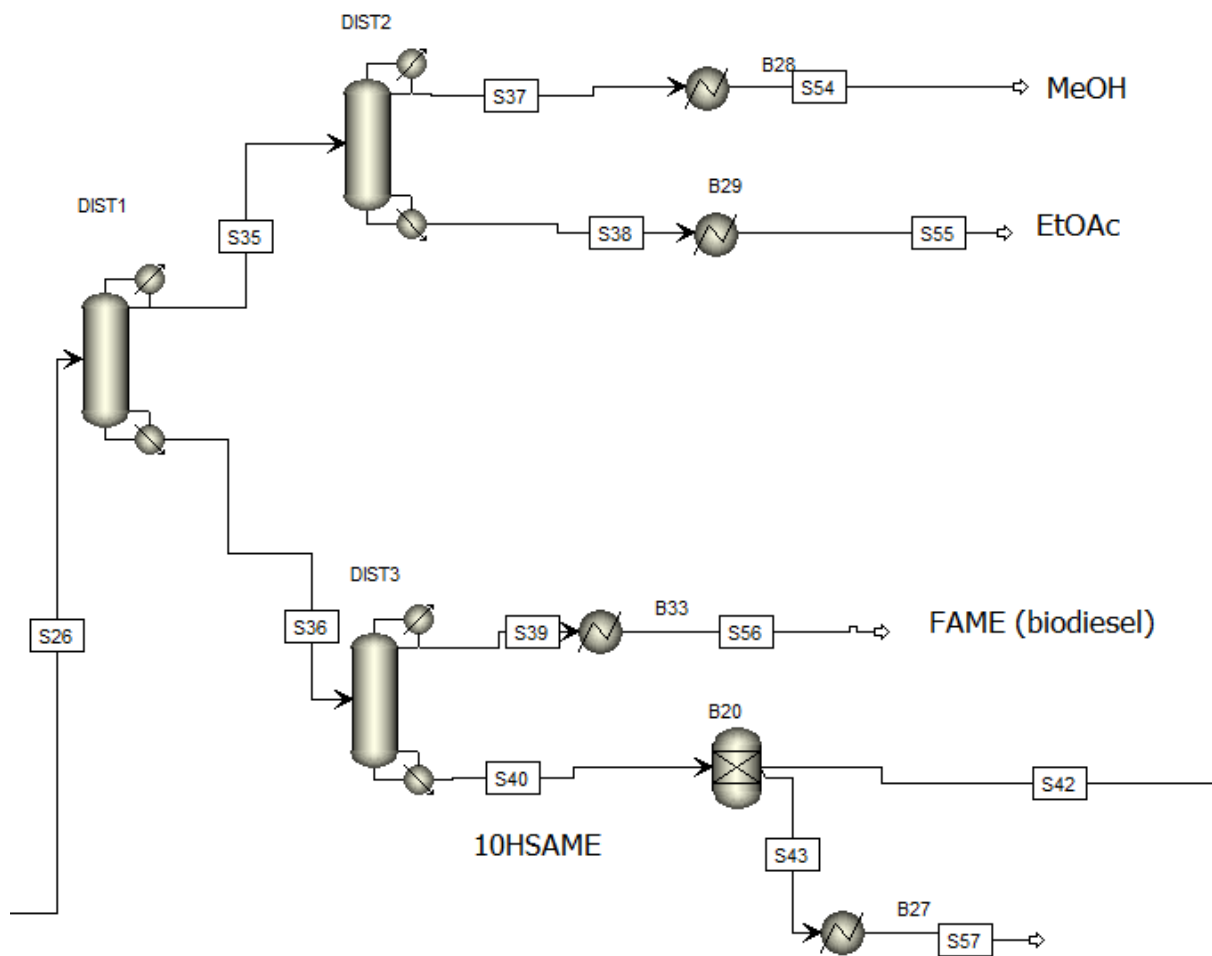


Figure 2.11: Aspen Plus flowsheet of the distillation process

2.3.6 Polymerization

The polymerization process utilizes the exit stream of the distillation process (DIST3) which contains a substantial amount of 10-HAME (S42) which is the key component needed to be later polymerized. Figure 2.12 includes the flow sheeting of the polymerization process conducted through Aspen Plus simulation engine. For the polymerization process, a decent amount of water is needed, while the use of a catalyst (DBTO) is obligated. The whole process is conducted under ambient pressure and high temperature of 350°C to secure the selectivity of the reaction. Neutral environment is also essential for the polymerization process, so for that cause a substantial amount of saturated N₂ is employed. Succeeding the polymerization process, methanol is produced and it is isolated through a flash reactor (FLASH2 or B12) due to the fact that it is volatile, to be recirculated for the esterification process in upcoming batches. After the polymerization process, a distillation column is implemented to recover the unreacted monomer in order to recirculate it back during the upcoming batch, enhancing the overall yield.

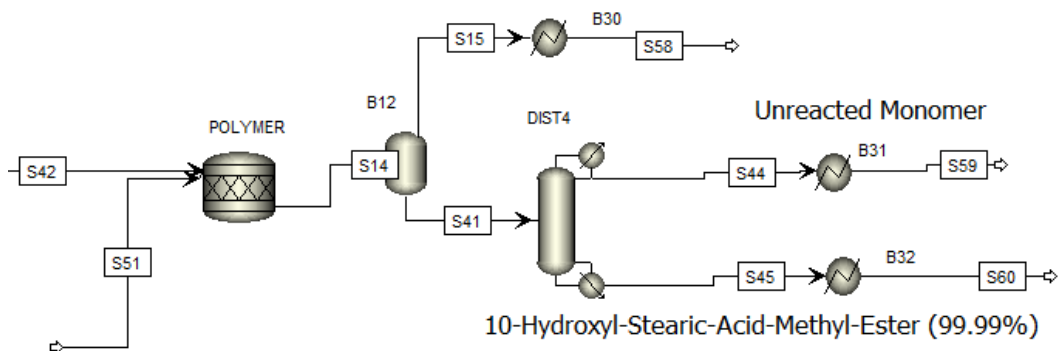


Figure 2.12: Depiction of the polymerization process derived from the Aspen Plus simulation engine

All the above modelling was conducted to obtain numerical results concerning the production of the bioplastic material. These results are summarized in the below *Table 2.12* regarding the most important components of the process.

Table 2.12: Primary inlets and outlets of the polymerization process

Compounds	Streams (kg/h)				
	S42	S51	S14	S59	S60
H2O	0	48	0	0	0
N2	0	2	2	0	2
10HSAME	1729.282	0	173.311	166.07	7.241
MEOH	0	0	170.746	0.2049	0
POLY	0	0	1553.212	1.550421	1548.87

2.4 ASPEN PROCESS MODELS

Transforming experimental data into scale-up process simulations is quite challenging in some cases. For instance, numerous assumptions and decisions have to be made in order to create an integrated simulation system. It should be noted that not every process simulation is perfectly created, the most important factor is to correctly evaluate the resulted estimations. Regarding the properties of the Aspen Plus modelling, numerous assumptions were made to build the data of components and thermodynamic methods. Various components necessary for the bio-chemical process were not included in the existing databases of Aspen Plus. For that reason, a chemical drawing of each or any of these components needed to be imported into the system, so that the simulation engine could calculate the desired chemical or physical quantity (e.g., Molecular weight or enthalpy of formation). In some cases, calculations may not be exactly accurate, for this cause, a series of calculations have to

be made in order to calculate the missing parameters and evaluate their estimation. It was also assumed that the starting oils contained only triglycerides based on oleic, linoleic, palmitic and stearic acid separately, meaning that one triglyceride consisted of only oleic acid chains, the other consisted of only linoleic acid chains etc. This assumption assisted in making the process simulation easier without having an impact on the estimated results. For the biorefinery process, a property method assistant was utilized to select the most appropriate thermodynamic method. NRTL was selected to contribute to calculating thermodynamic properties like Gibbs free energy, enthalpy or entropy.

During the main part of the whole undertaking, the simulation process, numerous assumptions were also made to obtain to previously noted results/estimations. One highly important assumption is that in Aspen Plus simulation, continuous processing was employed instead of batch processing to simplify the modelling. Moreover, Aspen Plus often assumes that there is negligible heat transfer occurring during the simulated system, to simplify the energy balances. Also, pressure drops across streams/pipes are often not considered important, because they do not significantly affect the calculations of the processing. To further investigate explicitly the assumptions made and the models utilized for the chemical simulation, a detailed representation of the models/assumptions made is depicted below:

1. Saponification/Acidification Process

Saponification and acidification processes are modelled utilizing RSTOIC stoichiometric reactors. Stream mixers are employed to combine the wanted streams in order to insert the desired components into the chemical reactors. The soaps produced from the saponification process needed to be drawn utilizing literature data regarding chemical information [38]. A flash reactor (FLASH2) is utilized to remove volatile components that imposed a problem during the upcoming liquid-liquid separation. A Decanter was used to separate the organic from the water phase, physically, to eventually result in the organic phase rich in FFAs.

2. Bio-catalysis Process

For the bio-catalysis process, RCSTR reactors were implemented that are based on known kinetic data retrieved from the previously conducted kinetic analysis. It was assumed that the bio-catalysis reaction is processed via a two-reactor stage to emphasize and estimate the results of the enzyme production and the enzymatic conversion of FFAs respectively. Normally, the bio-catalysis was conducted utilizing only one reactor both for the enzyme production and the conversion of FFAs, that assists in saving equipment and operation costs. To elaborate, biomass growth utilizes four different bioreactors that were not included in the simulation process, most of the enhancers/additives are included in the process flowchart only to indicate and estimate the cost of the raw materials because they act like catalyzers. Also, the created enzyme was imaginary, aiming to approach the properties of a real enzyme to make the whole bio-catalytic process more realistic. After the enzymatic conversion of FFAs, a separator (Sep) was processed like a membrane to remove the undesired enzyme continuing to the next steps of the process. The imaginary enzyme established serious simulation errors during the upcoming processes, so it needed to be isolated (in reality, the enzyme is not present in the exit stream of the bio-catalysis). Another separator was implemented to isolate various components that were not important/participating during the whole simulation and were only utilized as catalyzers throughout the saponification,

acidification and bio-catalysis process. A liquid-liquid separator (Decanter) was also utilized to further separate physically, the organic from the water phase. Regarding the upcoming spray dryer, a Flash2 was implemented to separate most of the ethyl acetate used from the unsaturated FFAs and water.

3. Hydrogeneration Process

For the hydrogeneration process, an RSTOIC model was developed to saturate the inserted FFAs. It was assumed that all the unsaturated FFAs and TGs were saturated evenly in a relatively high percentage. It is important to note that hydrogeneration normally occurs using a fixed bed reactor, with the addition of a nickel-based catalyst. The catalyst was not included in inlet stream for simplification purposes, though, it's considered in the total cost of raw materials during the upcoming TEA.

4. Esterification Process

The esterification process is manufactured via an RSTOIC model based on known stoichiometry. It should be stated that only the palmitic, stearic and 10-HA are esterified during the process, for simplification purposes. Oleic and linoleic acids are the only acids retrieved from the saponification/acidification process, that produce the key component of 10-HA, so the percentage of the unreacted oleic and linoleic acids is considered negligible. Thus, oleic and linoleic acids are not included in the esterification process, while a scarcely detectable amount is esterified in reality, contributing to the overall quantity of FAMES (biodiesel).

5. Distillation Process

In reality, a fractional distillation process is employed to separate the desired co-products. The three-stage distillation column process is used to simplify the process, without imposing a danger in false calculations. The designed columns utilized for the distillation process are DSTWU, which use the Winn-Underwood-Gilliland Method. A separator (Sep) is also implemented to upgrade the purities of the distillation process regarding the key product of 10-HAME.

6. Polymerization Process

Regarding the polymerization process, an RSTOIC model is developed based on known stoichiometric data. The most challenging part was to illustrate the produced biopolymer, in order to create a stoichiometric reaction. For this cause, the biopolymer was inserted into the system by importing/drawing the molecular structure as two connected 10-HAMEs. A Flash2 block was utilized to remove most of the methanol produced from the polymerization that created a simulation error during the upcoming distillation process. The distillation column (DSTWU) is utilized to separate the unreacted monomer from the biopolymer, to further recirculate the monomer to the next batch. A substantial amount of methanol is also retrieved from the underlying process and can be later exploited for the next esterification process.

2.5 WHOLE CHEMICAL PROCESS

All the above methodologies and procedures were conducted to create a fully integrated chemical process simulation. The exploitation of laboratory scale data was transformed into scaled-up processes to provide a deeper understanding of the philosophy of a biorefinery and the solutions that it provides for a more sustainable future. The below *Figure 2.13* and *Figure 2.14* illustrate the whole chemical process flowsheet, beginning with the Waste Cooking Oils and their treatment and the fermentation of *E. Coli* cells to eventually produce the biopolymer.

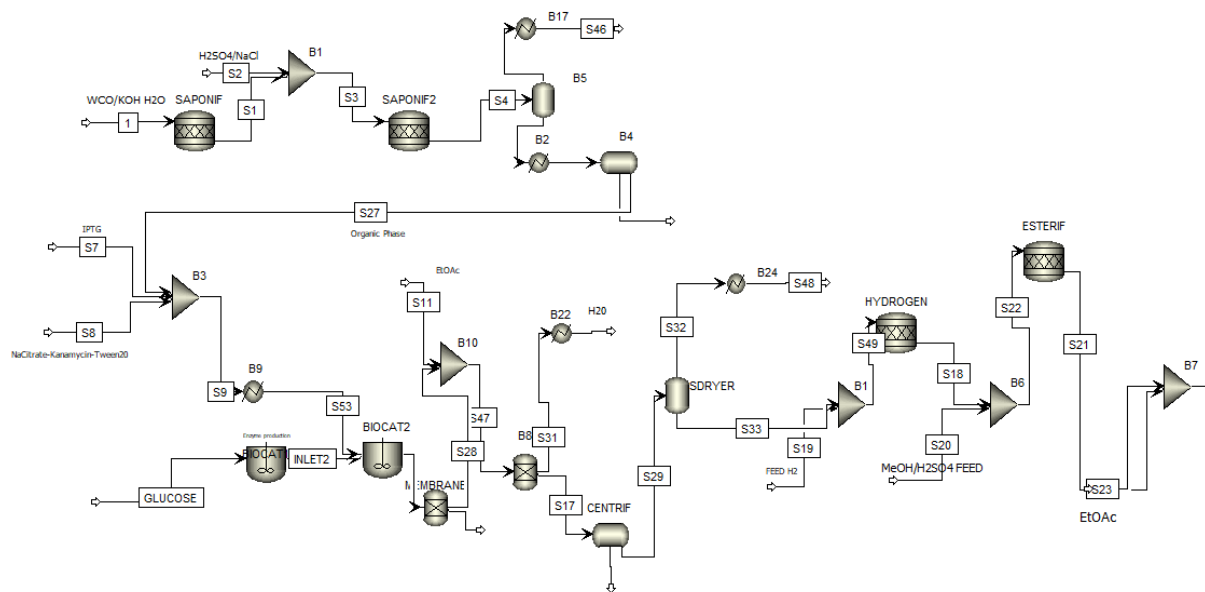


Figure 2.13: Illustration of the whole chemical process in Aspen Plus

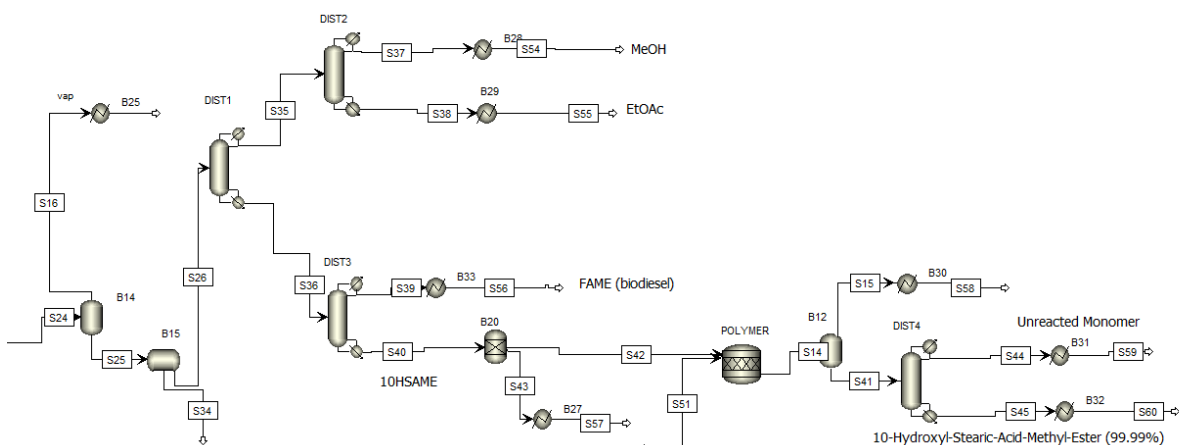


Figure 2.14: Illustration of the whole chemical process in Aspen Plus

2.6 RESULTS

The whole bio-catalytic process was conducted to determine and evaluate the results obtained from the process simulation analysis. Evaluating the laboratory scale outcomes, retrieved via Aspen Plus V11 simulation engine, provided scale-up estimations about the overall biochemical system. A summary of the main results of the process is obligatory to recapitulate the most important results of the process. *Table 2.13* provides a result compilation in comparison with experimental data to clarify the main results of each stage of the whole process.

Table 2.13: Comparison between experimental and simulation process yields of the key stages of the whole biocatalytic process

Processes	Experimental yields (%)	Simulation yield (%)
Saponification/Acidification	96	78.3
Bio-catalysis	80	86.4
Hydrogeneration	95	95
Esterification	95	85.9
Distillation	99	99.8
Polymerization	90	89.5
Overall	36.2	51.6

It is obvious that most of the yields differ from the experimental yields. This originates from the downstream processes' losses and the difference between a laboratory experiment and a scale-up simulation system. There is a great difference between the overall yield of the product in comparison with the most important raw materials (WCOs). It should be noted that the results retrieved from the computational analysis seem to be desired (realistic). To further elaborate, the assumptions made in order to create the process simulation play a major role in the evaluated results, thus creating a yield misbalance. Also, during the laboratory analysis, many different equipment tools were employed to conduct the experiments in correlation with the simulation analysis where the equipment, in certain cases, was completely different (e.g., centrifuge).

2.7 SENSITIVITY ANALYSIS

Sensitivity analysis often provides the examined chemical process with outstanding results when it comes to evaluating the perfect inputs to determine the most efficient and desired outcome. Various sensitivity analyses were conducted to determine and establish the most efficient amounts of compounds utilized in the most effective conditions. The whole analysis was conducted throughout Aspen Plus sensitivity analysis tool. For instance, the below *Figures 2.15-2.16* illustrate the main analyses derived from Aspen Plus sensitivity analysis tool to estimate the key parameters needed to obtain the optimum performance.

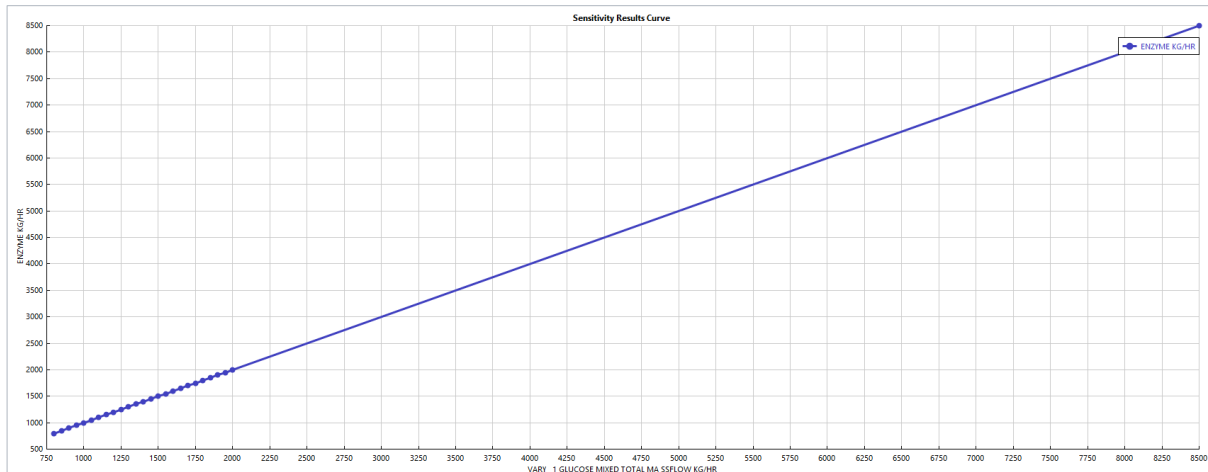


Figure 2.15: Sensitivity analysis that shows the correlation between the amount of glucose needed with the amount of the enzyme produced

It is concluded that the more glucose (substrate) used for the bio-catalysis step, the more enzyme is produced. This result is rational because during the Aspen Plus simulation analysis, the enzyme is produced from glucose, NO_2 and water.

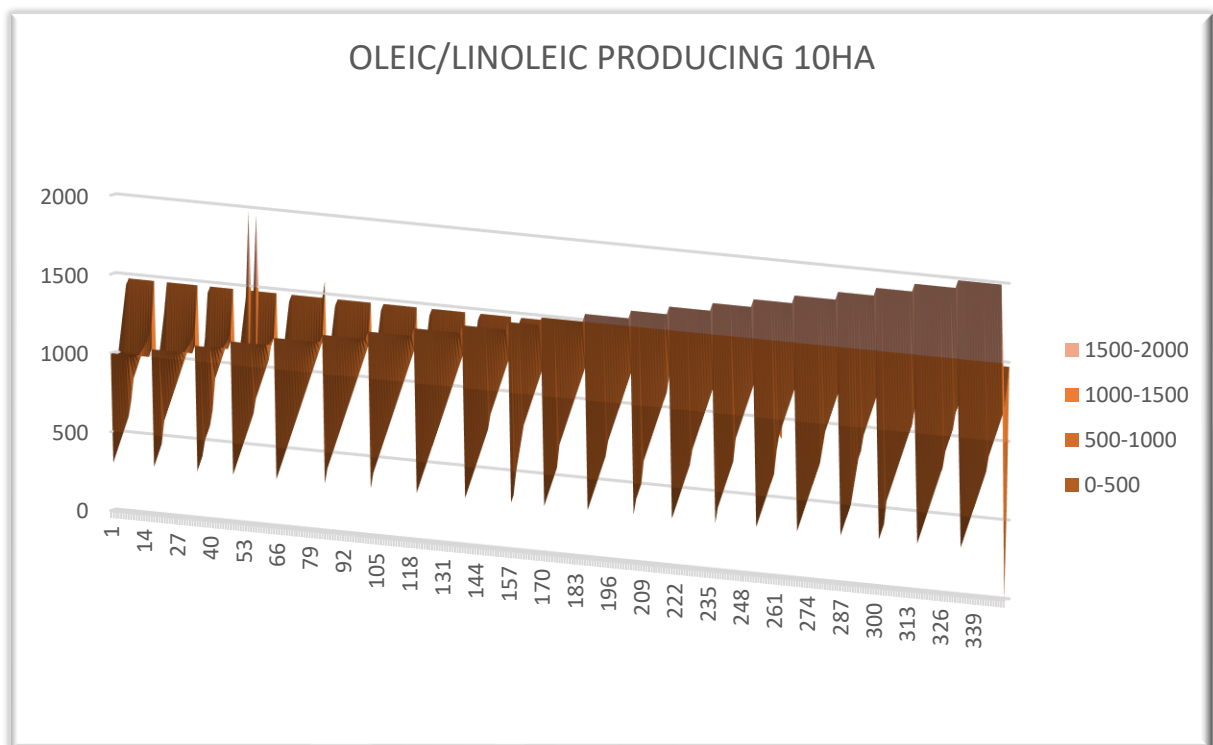


Figure 2.16: 3D Demonstration of the contribution of oleic and linoleic acid in producing 10-HA

The above Figure 2.16 presents the contribution of oleic and linoleic acids to produce 10-HA. The complicated diagram is a 3D demonstration that depicts the combined optimum feeds of oleic and

linoleic acids. To clarify, the optimum feeds occur in various proportions, one of which is obtained when oleic acid is around 1450 kg/h and linoleic acid is roughly at 600 kg/h. These results were utilized during the process simulation to obtain the best-case scenario (optimization).

2.8 ENERGY INTEGRATION

Energy integration in simulation processes can obtain extraordinary results and alternatives to reduce the energy usage of an industrial plant by employing the already existing heat and cold streams, as heat exchangers, for cooling down or heating up purposes respectively. Energy integration significantly minimizes the overall costs, otherwise the majority of biorefining concepts are threatened by reduced sustainability. The thermal data that were utilized to conduct the energy integration are listed in the below *Tables 2.14-2.15*.

Table 2.14: Thermal data utilized for the energy integration (Cold streams)

Cold streams		
T_{in} (°C)	T_{out} (°C)	Q [MW]
77.5	77.9	0.005
15	15.1	0.02
400	401	0.11
36.5	37	0.16
424	425	0.17
56.4	80	0.29
15	206.4	0.52
15	80	1.02
80	94.6	2.27
33.4	80	2.84

Table 2.15: Thermal data utilized for the energy integration (Hot streams)

Hot streams		
T_{in} (°C)	T_{out} (°C)	Q [MW]
37	15	6.9
94.6	15	2.3
94.6	15	2.1
515.8	15	0.47
77.9	15	0.38
350	349	0.35
37	36.9	0.24
123	122	0.23
206.4	15	0.23
217.6	15	0.19
37	15	0.19
194.2	150	0.15
77.9	15	0.14

367	366	0.07
37	36.9	0.07
350	15	0.04
236.2	15	0.02
47.1	15	0.02
68.9	15	0.003

Initially, the unintegrated hot and cold stream utilities consumption was 7.4 MW and 14.1 MW, respectively. After the energy integration, the total utilities were dramatically reduced to 2.24 MW (hot streams) and 8.9 MW (cold streams), which is equivalent to 70% and 37% (or 48% overall) of energy savings in heating and cooling demands. The optimal distribution over the utilities levels was accordingly estimated to 2.05 MW (LP steam), 0.19 (VHP steam) and 8.9 MW cooling water, as presented in the Grand Composite Curve depicted in *Figure 2.17*. It should be noted that the Grand Composite Curve is created, when following the methodology for energy integration utilizing the pinch analysis that was analysed during the previous Chapter 1.

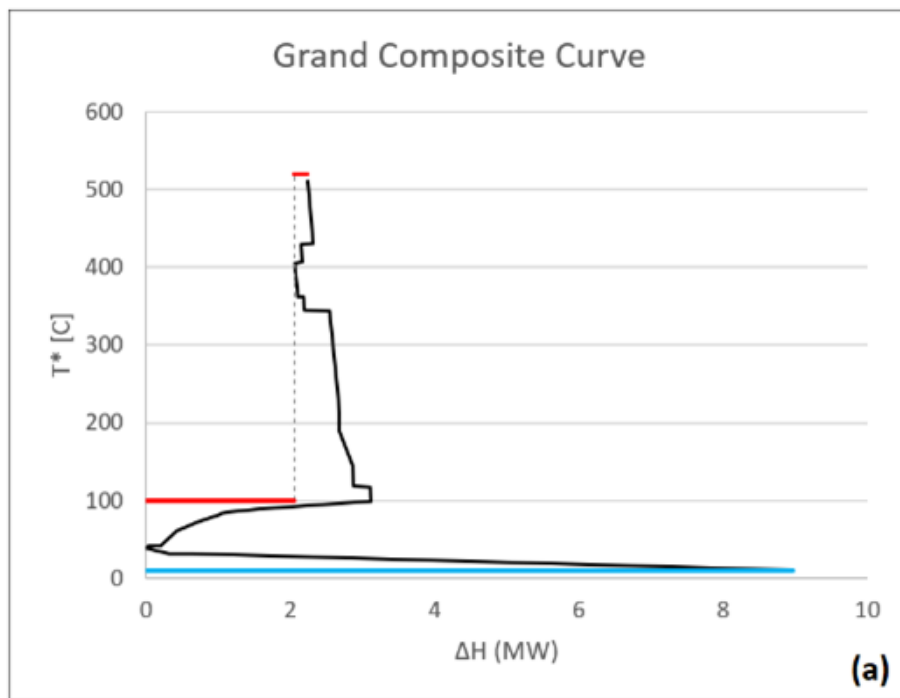


Figure 2.17: Grand Composite Curve retrieved from the energy integration

2.9 LIFE CYCLE ANALYSIS

On the other hand, Life Cycle Assessment (LCA) was conducted using SimaPro software to provide an estimation of the environmental impact of the biorefinery process. For the calculations, Ecoinvent databases were utilized seeking for environmental indicators, while the LCA procedure was completed in accordance with ReCiPe methods. For the LCA, all the quantities of the inputs and outputs of the

process simulation were exploited to finally estimate the environmental impact, that are illustrated in the below *Tables 2.16-2.17*.

Table 2.16: Inputs of the process simulation to estimate the environmental impact (LCA)

Inputs [kg/hr]	
Triolein	1,837
Trilinolein	750
Tripalmitin	226
KOH	637
H2O	20,859
ETHANOL	731
H2SO4	2,125
NaCl	477
Isopropyl β -d-1-thiogalactopyranoside	1.7
e.Coli	278
Polysorbate	0.0004
Kanamycin	0.1
Sodium Citrate	25
Ethyl Acetate	149
Methanol	408
Energy [MW]	2.2

Table 2.17: Outputs of the process simulation to estimate the environmental impact (LCA)

Outputs [kg/hr]	
Tristearin	87
Oleic acid	15
Linoleic acid	0.2
Palmitic acid	11
Stearic acid	20
Potassium oleate	8.3
Potassium linoleic	3.4
Potassium palmitate	22
Potassium stearate	234
H2O	285,413
KHSO4	1027
Glycerol	257
10-Hydroxyl-stearic-acid	82
Methyl stearate	378
Methyl palmitate	172
O2	24
Poly-10-HA	1424
Energy [MW]	9

The results of the LCA are presented in the below *Figure 2.18*, summarizing the significance of potential hazardous materials and the impact they could have on. In addition, Global Warming Potential (GWP) was calculated utilizing all the global warming gases like CO₂ produced by the biorefinery plant. This analysis provides a prompt environmental indication about whether the design of the plant is environmentally sustainable or not. It was concluded that, the emissions of CO₂ equivalent for the production of poly-10-HAME (biopolymer) were estimated around 2.4 kg CO₂eq/kg biopolymer, while the emissions for traditional fossil-based polymers covers a range of 2-3.5 kg CO₂eq/kg polymer.

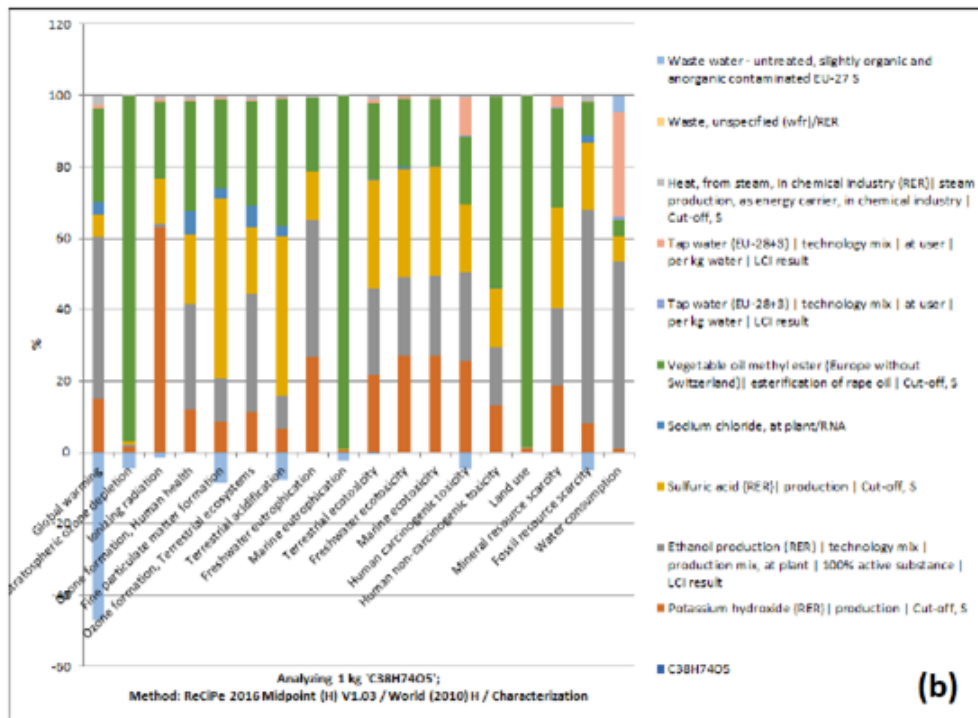


Figure 2.18: LCA results retrieved from the SimaPro software

2.10 TECHNO-ECONOMIC ANALYSIS

Every industry requires a Techno-Economic Analysis (TEA) to estimate financial indicators. The scaled-up simulation process also requires an economic analysis to evaluate the economic sustainability of such a biorefinery plant. Aspen Process Economic Analyzer (APEA) was utilized to approximate the capital and operating expenditures. Capital expenses like equipment cost are calculated from the program, while some of which could not be calculated (e.g., centrifuge). For this cause the equipment cost of some reactors/vessels had to be calculated, utilizing literature methodologies in calculating the equipment expenses based on the geometry, materials etc. [39]. Indicators like raw material expenses are also included in the overall TEA. The Capital Expenses (CAPEX) have been estimated to \$15.5M and include the equipment cost, cost for buildings (assets) etc., while the annual Operating Expenses (OPEX) are estimated to \$7.2M including all costs for materials, energy and auxiliary materials. As a result, for a depreciation period of 20 years, considering a (34-64%) cost allocation strategy an average price of 1.66 €/kg of biopolymer and 0.84€/kg of biopolymer could be achieved,

while respective market costs are identified to 0.91 €/kg (biodiesel) and 1.8 €/kg (PVC equivalent cost). Consequently, this analysis results in approximately 8% reduction of the selling price.

3 CONCLUSIONS

Valorization of waste and hazardous materials like WCOs will always be in the spotlight of the principles of green chemistry and circular economy. Finding ways to exploit materials that are often disposed, thus damaging the environment; could also provide economic benefits. Starting from used vegetable frying oils, this work presented a novel chemistry approach, enabling the valorization and upgrade of hazardous materials. The chemistry is attributed by complex kinetics explaining cellular growth of the bacteria *Escherichia Coli* that is fermented to produce an enzyme that catalyzes with enhanced selectivity the bio-catalysis reaction. The biorefinery plant utilizes the co-product (Biodiesel) to provide electrical and thermal energy to the system; thus, approaching a more sustainable and eco-friendly processing. Scaling-up the laboratory experimental data, exploiting Aspen Plus simulation engine, gave the opportunity to broaden the examined field by seeking ways to further integrate the biorefinery plant. Energy consumption reduction was achieved at a high percentage utilizing the pinch analysis. Environmental impacts were also decreased to establish a more sustainable biorefinery plant, in comparison with existing similar industries. An analysis, in terms of a financial perspective was conducted and examined to further estimate the economic sustainability of such an undertaking. In general, the idea of manipulating undesired raw material that is useless, hazardous and inexpensive in combination with exploiting microbial biomass to create a fully integrated process opens new pathways in chemical engineering. To conclude, this work managed to manufacture a completely integrated chemical process simulation, providing trusted results in terms of reaction yields, energy consumption, environmental impact and financial sustainability of the biorefinery plant.

SUGGESTIONS & FUTURE WORK

The current analysis objective is to fully integrate the simulation system and to deeply understand the kinetics of the most valuable process of the whole biorefinery project. Every process simulation has its drawbacks considering all the assumptions that were made to make this work possible. There is always room for improvement when it comes to scaling up a laboratory experiment to a process simulation system. It is suggested that an investigation seeking alternative auxiliaries (e.g., KOH), should be conducted to further reduce the environmental impact of their usage as well as to reduce the overall cost. Future work should also include alternative ways of downstream separations that could enhance the overall yield of the process, while decreasing or keeping the same equipment and operating cost (e.g., membranes). To elaborate, utilization of microorganisms and enzymatic conversions seem to be a great alternative that opens a wide range of fields that could be exploited in the future.

REFERENCES

1. Frota de Albuquerque Landi, Fabiana, et al. "Environmental Assessment of Four Waste Cooking Oil Valorization Pathways." *Waste Management*, vol. 138, Feb. 2022, pp. 219–233, <https://doi.org/10.1016/j.wasman.2021.11.037>. Accessed 3 Mar. 2022.
2. de Jong, Ed, and Gerfried Jungmeier. "Chapter 1 - Biorefinery Concepts in Comparison to Petrochemical Refineries." ScienceDirect, Elsevier, 1 Jan. 2015, www.sciencedirect.com/science/article/abs/pii/B978044463453500001X. Accessed 19 Apr. 2023.
3. Awogbemi, Omojola, et al. "Advances in Biotechnological Applications of Waste Cooking Oil." *Case Studies in Chemical and Environmental Engineering*, vol. 4, 1 Dec. 2021, p. 100158, www.sciencedirect.com/science/article/pii/S2666016421000803, <https://doi.org/10.1016/j.cscee.2021.100158>. Accessed 21 Dec. 2021.
4. EPA. "US EPA." US EPA, 2022, www.epa.gov/.
5. Wackett, L. P., and L. B. M. Ellis. "Biodegradation Database and Prediction, Microbial." ScienceDirect, Academic Press, 1 Jan. 2009, www.sciencedirect.com/science/article/abs/pii/B9780123739445002704. Accessed 19 Apr. 2023.
6. Kovárová-Kovar, Karin, and Thomas Egli. "Growth Kinetics of Suspended Microbial Cells: From Single-Substrate-Controlled Growth to Mixed-Substrate Kinetics." *Microbiology and Molecular Biology Reviews*, vol. 62, no. 3, 1 Sept. 1998, pp. 646–666, mmb.asm.org/content/62/3/646, <https://doi.org/10.1128/MMBR.62.3.646-666.1998>.
7. Lefebvre, Jérôme, et al. "Graphics-Associated Modeling of Batch Cultures of Escherichia Coli Fermenting Glucose." *Enzyme and Microbial Technology*, vol. 16, no. 2, Feb. 1994, pp. 163–169, [https://doi.org/10.1016/0141-0229\(94\)90080-9](https://doi.org/10.1016/0141-0229(94)90080-9). Accessed 7 Sept. 2022.
8. Wang, Hengwei, et al. "Improving the Expression of Recombinant Proteins in E. Coli BL21 (DE3) under Acetate Stress: An Alkaline PH Shift Approach." *PLoS ONE*, vol. 9, no. 11, 17 Nov. 2014, p. e112777, <https://doi.org/10.1371/journal.pone.0112777>. Accessed 7 Dec. 2021.
9. Pyrgakis, Konstantinos A., and Antonios C. Kokossis. "A Total Site Synthesis Approach for the Selection, Integration and Planning of Multiple-Feedstock Biorefineries." *Computers & Chemical Engineering*, vol. 122, Mar. 2019, pp. 326–355, <https://doi.org/10.1016/j.compchemeng.2018.09.003>. Accessed 3 Dec. 2020.
10. Kumar, Sunil. "Waste and the Environment: Underlying Burdens and Management Strategies." Elsevier, 2023, www.elsevier.com/books-and-journals/book-series/waste-and-the-environment-underlying-burdens-and-management-strategies.
11. Foo, Wei Han . "The Conundrum of Waste Cooking Oil: Transforming Hazard into Energy." *Journal of Hazardous Materials*, vol. 417, 5 Sept. 2021, p. 126129,

www.sciencedirect.com/science/article/pii/S0304389421010931,
<https://doi.org/10.1016/j.jhazmat.2021.126129>. Accessed 9 Aug. 2021.

12. Maotsela, Tlanelo, et al. "Utilization of Waste Cooking Oil and Tallow for Production of Toilet "Bath" Soap." *Procedia Manufacturing*, vol. 35, 2019, pp. 541–545, <https://doi.org/10.1016/j.promfg.2019.07.008>. Accessed 10 Jan. 2021.
13. "Elsevier Enhanced Reader." *Reader.elsevier.com*, 2021, reader.elsevier.com/reader/sd/pii/S2666016421000803?token=DFCAC9CE897AD8602156DAFBEBE44B09AA986E2CDC2A4ED48A79CF80C010E31F70F699756FAFA51BFAB0935393A1EEBA&originRegion=eu-west-1&originCreation=20230504111309. Accessed 4 May 2023.
14. Vassilev, Stanislav V., et al. "An Overview of the Chemical Composition of Biomass." *Fuel*, vol. 89, no. 5, May 2010, pp. 913–933, <https://doi.org/10.1016/j.fuel.2009.10.022>. Accessed 28 Mar. 2020.
15. Varbanov, Petar, et al. CHEMICAL ENGINEERING TRANSACTIONS Cooking Oil and Fat Waste Management: A Review of the Current State. 2020, www.aidic.it/cet/20/81/128.pdf, <https://doi.org/10.3303/CET2081128>.
16. Taylor, Hugh S. "Catalysis | Chemistry, Classification, & Chemical Reactions." *Encyclopædia Britannica*, 30 July 2018, www.britannica.com/science/catalysis.
17. Robinson, Peter. "Enzymes: Principles and Biotechnological Applications." *Essays in Biochemistry*, vol. 59, no. 59, 15 Nov. 2015, pp. 1–41, www.ncbi.nlm.nih.gov/pmc/articles/PMC4692135/, <https://doi.org/10.1042/bse0590001>.
18. Center for Food Safety and Applied Nutrition. "Escherichia Coli (E. Coli)." U.S. Food and Drug Administration, 2019, www.fda.gov/food/foodborne-pathogens/escherichia-coli-e-coli.
19. "Catalytic Hydrogenation of Alkenes." *Chemistry LibreTexts*, 2 Oct. 2013, chem.libretexts.org/Bookshelves/Organic_Chemistry/Supplemental_Modules_%28Organic_Chemistry%29/Alkenes/Reactivity_of_Alkenes/Catalytic_Hydrogenation.
20. Britannica. "Distillation | Chemical Process." *Encyclopædia Britannica*, 2019, www.britannica.com/science/distillation.
21. ---. "Polymerization | Chemical Reaction." *Encyclopædia Britannica*, 6 Apr. 2016, www.britannica.com/science/polymerization.
22. Kasmi, Nejib, et al. "Solid-State Polymerization of Poly(Ethylene Furanoate) Biobased Polyester, I: Effect of Catalyst Type on Molecular Weight Increase." *Polymers*, vol. 9, no. 11, 13 Nov. 2017, p. 607, <https://doi.org/10.3390/polym9110607>. Accessed 30 Oct. 2022.
23. "27.8: Polymers and Polymerization Reactions." *Chemistry LibreTexts*, 18 Jan. 2015, chem.libretexts.org/Bookshelves/General_Chemistry/Map%3A_General_Chemistry_%28Petrucci_et_al.%29/27%3A_Reactions_of_Organic_Compounds/27.08%3A_Polymers_and_Polymerization_Reactions.

24. The World Counts. "The World Counts." [Www.theworldcounts.com](http://www.theworldcounts.com), 2023, www.theworldcounts.com/challenges/planet-earth/waste/global-waste-problem.
25. Mendow, G., et al. "Ethyl Ester Production by Homogeneous Alkaline Transesterification: Influence of the Catalyst." *Bioresource Technology*, vol. 102, no. 11, 1 June 2011, pp. 6385–6391, pubmed.ncbi.nlm.nih.gov/21339065/, <https://doi.org/10.1016/j.biortech.2011.01.072>.
26. Jove. "Esterification | Protocol." [Www.jove.com](http://www.jove.com), www.jove.com/science-education/11219/esterification.
27. Cruz, Mariana, et al. "RECOVERY of BY-PRODUCTS from the OLIVE OIL PRODUCTION and the VEGETABLE OIL REFINING for BIODIESEL PRODUCTION." *Detritus*, vol. In Press, no. 0, 2018, p. 1, <https://doi.org/10.31025/2611-4135/2018.13728>.
28. Mannu, Alberto, et al. "Available Technologies and Materials for Waste Cooking Oil Recycling." *Processes*, vol. 8, no. 3, 22 Mar. 2020, p. 366, <https://doi.org/10.3390/pr8030366>.
29. RIERA, José BOATELLA, and Rafael CODONY. "RECYCLED COOKING OILS : ASSESSMENT of RISKS for PUBLIC HEALTH Final Study." *Semantic Scholar, European Parliament Directorate General for Research Directorate A The STOA Programme*, Sept. 2000, www.semanticscholar.org/paper/RECYCLED-COOKING-OILS-%3A-ASSESSMENT-OF-RISKS-FOR/c52f242121f516f39cbe01276ec63c9b8d25a504. Accessed 16 May 2023.
30. McDaniel, L. E., et al. "Effect of Oxygen-Supply Rates on Growth of Escherichia Coli." *Applied Microbiology*, vol. 13, no. 1, 1965, pp. 109–114, <https://doi.org/10.1128/am.13.1.109-114.1965>. Accessed 5 Feb. 2021.
31. Paalme, T., et al. "The Growth Rate Control in Escherichia Coli at near to Maximum Growth Rates: The A-Stat Approach." *Antonie van Leeuwenhoek*, vol. 71, no. 3, 1997, pp. 217–230, <https://doi.org/10.1023/a:1000198404007>. Accessed 22 Oct. 2020.
32. Marr, Allen G., and John L. Ingraham. "EFFECT of TEMPERATURE on the COMPOSITION of FATTY ACIDS in ESCHERICHIA COLI." *Journal of Bacteriology*, vol. 84, no. 6, 1962, pp. 1260–1267, <https://doi.org/10.1128/jb.84.6.1260-1267.1962>.
33. Kovárová, K, et al. "Temperature-Dependent Growth Kinetics of Escherichia Coli ML 30 in Glucose-Limited Continuous Culture." *Journal of Bacteriology*, vol. 178, no. 15, Aug. 1996, pp. 4530–4539, <https://doi.org/10.1128/jb.178.15.4530-4539.1996>.
34. Wyman, Charles E., et al. "Coordinated Development of Leading Biomass Pretreatment Technologies." *Bioresource Technology*, vol. 96, no. 18, Dec. 2005, pp. 1959–1966, <https://doi.org/10.1016/j.biortech.2005.01.010>. Accessed 9 Dec. 2021.
35. Hassan, Shady S., et al. "Lignocellulosic Biorefineries in Europe: Current State and Prospects." *Trends in Biotechnology*, vol. 37, no. 3, Mar. 2019, pp. 231–234, <https://doi.org/10.1016/j.tibtech.2018.07.002>. Accessed 4 Nov. 2020.

36. Foo, Wei Han, et al. "Recent Advances in the Conversion of Waste Cooking Oil into Value-Added Products: A Review." *Fuel*, vol. 324, 15 Sept. 2022, p. 124539, www.sciencedirect.com/science/article/pii/S0016236122013886, <https://doi.org/10.1016/j.fuel.2022.124539>.
37. March, Linnhoff. *Introduction to Pinch Technology*. 1998.
38. PubChem. "The PubChem Project." Nih.gov, National Library of Medicine, 2022, pubchem.ncbi.nlm.nih.gov/.
39. James Merrill Douglas. *Conceptual Design of Chemical Processes*. McGraw-Hill Science, Engineering & Mathematics, 1988.

APPENDIX A: PROCESS SIMULATION

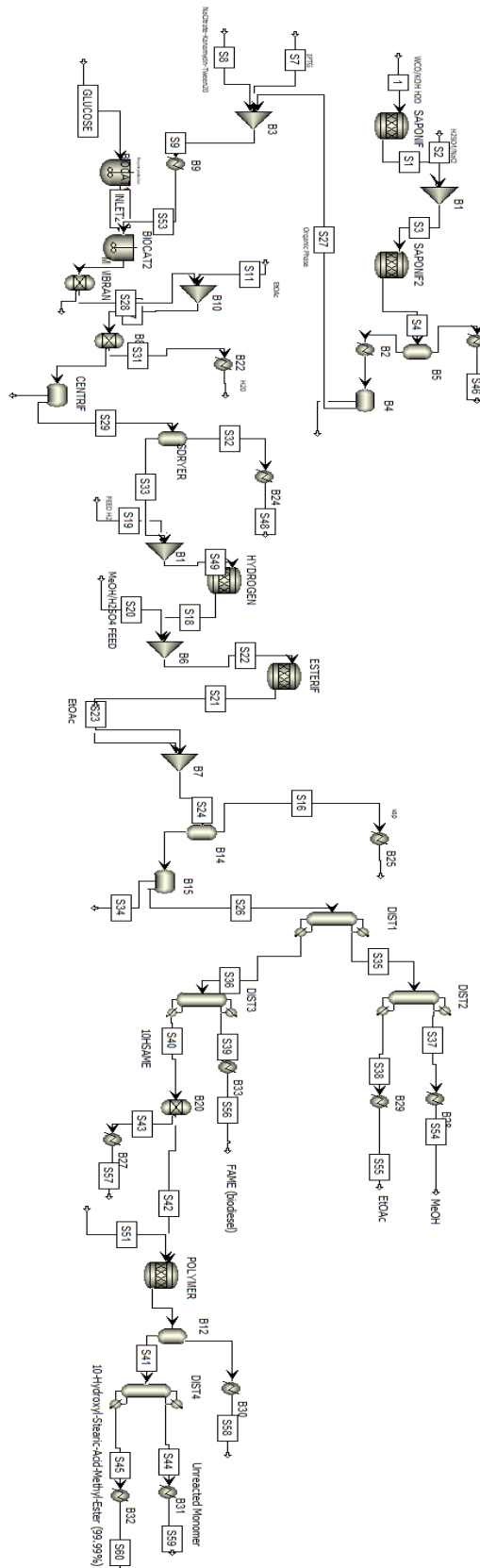


Figure 3.1: Schematization of the whole chemical process simulation